

A Subsampling Line-Search Method with Second-Order Results

E. Bergou^{*} Y. Diouane[†] V. Kunc[‡] V. Kungurtsev[§] C. W. Royer[¶]

July 1, 2021

Abstract

In many contemporary optimization problems such as those arising in machine learning, it can be computationally challenging or even infeasible to evaluate an entire function or its derivatives. This motivates the use of stochastic algorithms that sample problem data, which can jeopardize the guarantees obtained through classical globalization techniques in optimization such as a line search. Using subsampled function values is particularly challenging for the latter strategy, which relies upon multiple evaluations. For nonconvex data-related problems, such as training deep learning models, one aims at developing methods that converge to second-order stationary points quickly, i.e., escape saddle points efficiently. This is particularly difficult to ensure when one only accesses subsampled approximations of the objective and its derivatives.

In this paper, we describe a stochastic algorithm based on negative curvature and Newton-type directions that are computed for a subsampling model of the objective. A line-search technique is used to enforce suitable decrease for this model, and for a sufficiently large sample, a similar amount of reduction holds for the true objective. We then present worst-case complexity guarantees for a notion of stationarity tailored to the subsampling context. Our analysis encompasses the deterministic regime, and allows us to identify sampling requirements for second-order line-search paradigms. As we illustrate through real data experiments, these worst-case estimates need not be satisfied for our method to be competitive with first-order strategies in practice.

Keywords: Nonconvex optimization; finite-sum problems; subsampling methods; negative curvature; worst-case complexity.

^{*}MaIAGE, INRAE, Université Paris-Saclay, 78350 Jouy-en-Josas, France (elhoucine.bergou@inra.fr). King Abdullah University of Science and Technology (KAUST), Thuwal, Saudi Arabia. This author received support from the AgreeSkills+ fellowship programme which has received funding from the EU's Seventh Framework Programme under grant agreement No FP7-609398 (AgreeSkills+ contract).

[†]ISAE-SUPAERO, Université de Toulouse, 31055 Toulouse Cedex 4, France (youssef.diouane@isae.fr).

[‡]Department of Computer Science, Faculty of Electrical Engineering, Czech Technical University in Prague (kuncvlad@fel.cvut.cz). Support for this author was provided by the CTU SGS grant no. SGS17/189/OHK3/3T/13.

[§]Department of Computer Science, Faculty of Electrical Engineering, Czech Technical University in Prague (vyacheslav.kungurtsev@fel.cvut.cz). Support for this author was provided by the OP VVV project CZ.02.1.01/0.0/0.0/16_019/0000765 "Research Center for Informatics".

[¶]LAMSADE, CNRS, Université Paris-Dauphine, Université PSL, 75016 PARIS, FRANCE (clement.royer@dauphine.psl.eu). Support for this author was partially provided by Subcontract 3F-30222 from Argonne National Laboratory.

1 Introduction

In this paper, we aim to solve

$$\min_{x \in \mathbb{R}^n} f(x) := \frac{1}{N} \sum_{i=1}^N f_i(x), \quad (1)$$

where the objective function f is not necessarily convex and the components f_i are assumed to be twice-continuously differentiable on \mathbb{R}^n . We are interested in problems in which the number of components $N \geq 1$ is extremely large, so that it becomes computationally infeasible to evaluate the entire function, its gradient or its Hessian.

To overcome this issue, we consider the use of *subsampling techniques* to compute stochastic estimates of the objective function, its gradient and its Hessian. Given a random set \mathcal{S} sampled from $\{1, \dots, N\}$ and a point $x \in \mathbb{R}^n$, we use the following estimates of f and its derivatives:

$$\hat{f}(x; \mathcal{S}) := \frac{1}{|\mathcal{S}|} \sum_{i \in \mathcal{S}} f_i(x), \quad g(x; \mathcal{S}) := \frac{1}{|\mathcal{S}|} \sum_{i \in \mathcal{S}} \nabla f_i(x), \quad H(x; \mathcal{S}) := \frac{1}{|\mathcal{S}|} \sum_{i \in \mathcal{S}} \nabla^2 f_i(x), \quad (2)$$

where $|\mathcal{S}|$ denotes the cardinal number of the sampling set \mathcal{S} . We are interested in iterative minimization procedures that choose a new random sampling set \mathcal{S} at every iteration.

The standard subsampling optimization procedure for such a problem is the (batch) stochastic gradient descent (SGD) method, wherein the gradient is estimated by one component gradient ∇f_i (or a batch of component), and a step is taken in the negative of this direction. The SGD framework is ubiquitous in a variety of applications, including large-scale machine learning problems, particularly those arising from the training of deep neural net architectures [11]. However, it is known to be sensitive to nonconvexity, particularly in the context of training deep neural nets. For such problems, it has indeed been observed that the optimization landscape for the associated (nonconvex) objective exhibits a significant number of saddle points, around which the flatness of the function tends to slow down the convergence of SGD [20]. This behavior is typical of first-order methods, despite the fact that those schemes almost never converge to saddle points [31]. By incorporating second-order information, one can guarantee that saddle points can be escaped from at a favorable rate: various algorithms that provide such guarantees while only requiring gradient or Hessian-vector products have been proposed in the literature [1, 2, 32, 48]. Under certain accuracy conditions, which can be satisfied with arbitrarily high probability by controlling the size of the sample, these methods produce a sequence of iterates that converge to a local minimizer at a certain rate. Alternatively, one can extract second-order information and escape saddle points using accelerated gradient techniques in the stochastic setting [43]. The results are also in high probability, with a priori tuned stepsizes. Noise can be used to approximate second-order information as well [48]. Recent proposals [46, 49] derive high probability convergence results with second-order steps (e.g., Newton steps) based on sampled derivatives and exact objective values, by means of trust-region and cubic regularization frameworks. Stochastic subsampling Newton methods, including [5, 9, 13, 22, 36, 39, 47], exploit second-order information to accelerate the convergence while typically using a line search on exact function values to ensure global convergence. In the general stochastic optimization setting, a variety of algorithms have been extended to handle access to sampled derivatives, and possibly function values: of particular interest to us are the algorithms endowed with complexity guarantees. When exact function values can be computed, one can employ strategies based on line search [16], cubic regularization [16, 27] or trust region [19, 24] to compute a step of suitable

length. Many algorithms building on SGD require the tuning of the step size parameter (also called learning rate), which can be cumbersome without knowledge of the Lipschitz constant. On the contrary, methods that are based on a globalization technique (line search, trust region, quadratic or cubic regularization) can control the size of the step in an adaptive way, and are thus less sensitive to parameter tuning.

In spite of their attractive properties with respect to the step size, globalized techniques are challenging to extend to the context of inexact function values. Indeed, these methods traditionally accept new iterates only if they produce a sufficient reduction of the objective value. Nevertheless, inexact variants of these schemes have been a recent topic of interest in the literature. In the context of stochastic optimization, several trust-region algorithms that explicitly deal with computing stochastic estimates of the function values have been described [8, 18, 29]. In the specific case of least-squares problems, both approaches (exact and inexact function values) have been incorporated within a Levenberg-Marquardt framework [6, 7]. The use of stochastic function estimates in a line-search framework (a process that heavily relies on evaluating the function at tentative points) has also been the subject of very recent investigation. A study based on proprietary data [28] considered an inexact Newton and negative curvature procedure using each iteration’s chosen mini-batch as the source of function evaluation sample in the line search. A stochastic line-search technique was introduced in [33], where extensive experiments matching performance to pre-tuned SGD were presented. An innovating technique based on a backtracking procedure for steps generated by a limited memory BFGS method for nonconvex problems using first-order information was recently proposed in [10], and first-order convergence results were derived. Finally, contemporary to the first version of this paper, a stochastic line-search framework was described by [35]. Similarly to our scheme, this algorithm computes stochastic estimates for function and gradient values, which are then used within a line-search algorithm. However, the two methods differ in their inspiration and results: we provide more details about these differences in the next paragraph, and throughout the paper when relevant.

In this paper, we propose a line-search scheme with second-order guarantees based on subsampling function and derivative evaluations. Our method uses these subsampled values to compute Newton-type and negative curvature steps. Although our framework bears similarities with the approach of [35], the two algorithms are equipped with different analyzes, each based on their own arguments from probability theory. The method of [35] is designed with first-order guarantees in mind (in particular, the use of negative curvature is not explored), and its complexity results are particularized to the nonconvex, convex and strongly convex cases; our work presents a line-search method that is dedicated to the nonconvex setting, and to the derivation of second-order results. Earlier work on second-order guarantees for subsampling methods often focused on complexity bounds holding with a high probability (of accurate samples being taken at each iteration), disallowing poor outlier estimates of the problem function. Our results are complementary as we establish a rate of convergence to points satisfying approximate second-order optimality conditions in expectation. In addition to theoretical results, we test an implementation of our method on contemporary neural network training tasks, and compare it with a stochastic gradient approach using the same amount of sampling. Our results indicate that the proposed method performs well when these problems involve a large amount of data but a small number of parameters. Although the case of a large number of parameters require a careful implementation, we provide insights regarding the promises of our second-order technique.

We organize this paper as follows. In Section 2, we describe our proposed approach based on line-search techniques. In Section 3, we derive bounds on the amount of expected decrease that can be achieved at each iteration by our proposed approach. Section 4 gives the global convergence rate of our method under appropriate assumptions, followed by a discussion about the required properties and their satisfaction in practice. A numerical study of our approach is provided in Section 5. A discussion of conclusions and future research is given in Section 6.

Throughout the paper, $\|\cdot\|$ denotes the Euclidean norm. A vector $v \in \mathbb{R}^n$ will be called a unit vector if $\|v\| = 1$. Finally, \mathbb{I}_n denotes the identity matrix of size n .

2 Subsampling line-search method

In this section, we introduce a line-search algorithm dedicated to solving the unconstrained optimization problem (1): the detailed framework is provided in Algorithm 1. At each iteration k , our method computes a random sampling set \mathcal{S}_k , and the associated estimates $g_k := g(x_k; \mathcal{S}_k)$ and $H_k := H(x_k; \mathcal{S}_k)$ of $\nabla f(x_k)$ and $\nabla^2 f(x_k)$, respectively. Since we have computed \mathcal{S}_k , the model $\hat{f}_k(\cdot) := \hat{f}(\cdot; \mathcal{S}_k)$ of the function f is also defined: the estimates $g_k := g(x_k; \mathcal{S}_k)$ and $H_k := H(x_k; \mathcal{S}_k)$ define the quadratic Taylor expansion of \hat{f}_k around x_k , which we use to compute a search direction d_k . The form of this direction is set based on the norm of g_k as well as the minimum eigenvalue of H_k , denoted by λ_k . The process is described through Steps 2-5 of Algorithm 1, and involves an optimality tolerance ϵ . When $\lambda_k < -\epsilon$, the Hessian estimate is indefinite, and we choose to use a negative curvature direction, as we know that it will offer sufficient reduction in the value of \hat{f}_k (see the analysis of Section 3.2). When $\lambda_k \geq \|g_k\|^{1/2}$, the quadratic function defined by g_k and H_k is (sufficiently) positive definite, and this allows us to compute and use a Newton direction. Finally, when $\lambda_k \in [-\epsilon^{1/2}, \|g_k\|^{1/2}]$, we regularize this quadratic by an amount of order $\epsilon^{1/2}$, so that we fall back into the previous case: we thus compute a regularized Newton direction, for which we will obtain desirable decrease properties. Once the search direction has been determined, and regardless of its type, a backtracking line-search strategy is applied to select a step size α_k that decreases the model \hat{f}_k by a sufficient amount (see condition (7)). This condition is instrumental in obtaining good complexity guarantees.

Aside from the use of subsampling, Algorithm 1 differs from the original method of [41] in two major ways. First, we only consider three types of search direction, as opposed to five in the original method of [41]. Indeed, in order to simplify the upcoming theoretical analysis, we do not allow for selecting gradient-based steps, i.e. steps that are colinear with the negative (subsampled) gradient. Note that such steps do not affect the complexity guarantees, but have a practical value since they are cheaper to compute. For this reason, we present the algorithm without their use, but we will re-introduce them in our numerical experiments. Secondly, our strategy for choosing among the three different forms for the direction differs slightly from [41] in the “if” condition in Step 4 of the algorithm and in the regularization used for the regularized Newton, see equation (6). In Section 4, we will show that such algorithmic modifications will lead also to results that are equivalent to those of the original deterministic method [41]. Nevertheless, and for the reasons already mentioned in the first point, we will also revert to the original rule in our practical implementation (see Section 5.1).

Three comments about the description of Algorithm 1 are in order. First, we observe that the method as stated is not equipped with a stopping criterion. Apart from budget considerations, one might be tempted to stop the method when the derivatives are suggesting that it is a

Algorithm 1: A Line-search Algorithm based on Subsampling (ALAS).

Initialization: Choose $x_0 \in \mathbb{R}^n$, $\theta \in (0, 1)$, $\eta > 0$, $\epsilon > 0$.

for $k = 0, 1, \dots$ **do**

1. Draw a random sample set $\mathcal{S}_k \subset \{1, \dots, N\}$, and compute the associated quantities $g_k := g(x_k; \mathcal{S}_k)$, $H_k := H(x_k; \mathcal{S}_k)$. Form the estimation \hat{f}_k as a function of the variable s :

$$\hat{f}_k(x_k + s) := \hat{f}(x_k + s; \mathcal{S}_k). \quad (3)$$

2. Compute λ_k as the minimum eigenvalue of the Hessian estimate H_k .
If $\lambda_k \geq -\epsilon^{1/2}$ and $\|g_k\| = 0$ set $\alpha_k = 0$, $d_k = 0$ and go to Step 7.

3. If $\lambda_k < -\epsilon^{1/2}$, compute a negative eigenvector v_k such that

$$H_k v_k = \lambda_k v_k, \quad \|v_k\| = -\lambda_k, \quad v_k^\top g_k \leq 0, \quad (4)$$

set $d_k = v_k$ and go to the line-search step.

4. If $\lambda_k > \|g_k\|^{1/2}$, compute a Newton direction d_k solution of

$$H_k d = -g_k, \quad (5)$$

go to the line-search step.

5. If d_k has not yet been chosen, compute it as a regularized Newton direction, solution of

$$\left(H_k + (\|g_k\|^{1/2} + \epsilon^{1/2}) \mathbb{I}_n \right) d_k = -g_k, \quad (6)$$

and go to the line-search step.

6. **Line-search step** Compute the minimum index j_k such that the step length $\alpha_k := \theta^{j_k}$ satisfies the decrease condition:

$$\hat{f}_k(x_k + \alpha_k d_k) - \hat{f}_k(x_k) \leq -\frac{\eta}{6} \alpha_k^3 \|d_k\|^3. \quad (7)$$

7. Set $x_{k+1} = x_k + \alpha_k d_k$.

8. Set $k = k + 1$.

end

second-order stationary point. However, since we only have access to subsampled versions of those derivatives, it is possible that we have not reached a stationary point for the true function. As we will establish later in the paper, one needs to take into account the accuracy of the model, and it might take several iterations to guarantee that we are indeed at a stationary point. We discuss the link between stopping criteria and stationarity conditions in Section 4.

Our second remark relates to the computation of a step. When the subsampled gradient g_k is zero and the subsampled matrix H_k is positive definite, we cannot compute a descent step using first- or second-order information, because the current iterate is second-order stationary for the subsampled model. In that situation, and for the reasons mentioned in the previous paragraph, we do not stop our method, but rather take a zero step and move on to a new iteration and a new sample set. After a certain number of such iterations, one can guarantee that a stationary

point has been reached with high probability (see Section 4).

The third remark is about the size of the random sample that we did not specify. The algorithm supports adaptive sample size. For the sake of simplicity and clarity, in our theoretical analysis (see Theorem 1) we focus on using a lower bound which is independent from k . This bound on the sample size depends on ϵ but is limited by the full sample size (see Condition (21)). One may derive a sharper lower bound on the sample size, but such a bound will involve random, iteration-dependent quantities, which introduces a number of measurability issues. We thus chose to focus on constant bounds on the sample size.

3 Expected decrease guarantees with subsampling

In this section, we derive bounds on the amount of expected decrease at each iteration. When the current sample leads to good approximations of the objective and derivatives, we are able to guarantee decrease in the function for any possible step taken by Algorithm 1. By controlling the sample size, one can adjust the probability of having a sufficiently good model, so that the guaranteed decrease for good approximations will compensate a possible increase for bad approximations on average.

3.1 Preliminary assumptions and definitions

Throughout the paper, we will study Algorithm 1 under the following assumptions.

Assumption 3.1 *The function f is bounded below by $f_{\text{low}} \in \mathbb{R}$.*

Assumption 3.2 *The functions f_i are twice continuously differentiable, with Lipschitz continuous gradients and Hessians, of respective Lipschitz constants L_i and $L_{H,i}$.*

A consequence of Assumption 3.2 is that f is twice continuously differentiable, Lipschitz, with Lipschitz continuous first and second-order derivatives. This property also holds for $m(\cdot; \mathcal{S})$, regardless of the value of \mathcal{S} (we say that the property holds *for all realizations of \mathcal{S}*). In what follows, we will always consider that $m(\cdot; \mathcal{S})$ and f have L -Lipschitz continuous gradients and L_H -Lipschitz continuous Hessians, where $L := \max_i L_i$ and $L_H := \max_i L_{H,i}$. Another corollary of Assumption 3.2 is that there exists a finite positive constant U_H such that $U_H \geq \max_{i=1, \dots, N} \|\nabla^2 f_i(x_k)\|$ for every k . The value $L = U_H$ is a valid one, however we make the distinction between the two by analogy with previous works [41, 46]. In the same spirit, we make the following additional assumption.

Assumption 3.3 *There exists a finite positive constant U_g such that,*

$$U_g \geq \max_{i=1, \dots, N} \|\nabla f_i(x_k)\| \quad \forall k,$$

for all realizations of the algorithm.

Assumption 3.3 guarantees that every trial step will be bounded in norm, and that the possible increase of f produced by this step will also be bounded. Note that such assumption is less restrictive than assuming that all f_i 's are Lipschitz continuous, or that there exists a compact set that contains the sequence of iterates. The satisfaction of such assumption can be

ensured in practice by restarting the method whenever the algorithm detects unboundedness of the iterates, which never occurred in our numerical experiments. Besides, because our sampling set is finite, the set of possibilities for each iterate is bounded (though it grows at a combinatorial pace).

In the rest of the analysis, for every iteration k , we let $\pi_k := \frac{|\mathcal{S}_k|}{N}$ denote the *sample fraction* used at every iteration. Our objective is to identify threshold values on π_k that lead to (expected) decrease in the objective.

Whenever the sample sets in Algorithm 1 are drawn at random, the subsampling process introduces randomness in an iterative fashion at every iteration. As a result, Algorithm 1 results in a stochastic process $\{x_k, d_k, \alpha_k, g_k, H_k, \hat{f}_k(x_k), \hat{f}_k(x_k + \alpha_k d_k)\}$ (we point out that the sample fractions need not be random). To lighten the notation throughout the paper, we will use these notations for the random variables and their realizations. Most of our analysis will be concerned with random variables, but we will explicitly mention that realizations are considered when needed. Our goal is to show that under certain conditions on the sequences $\{g_k\}$, $\{H_k\}$, $\{\hat{f}_k(x_k)\}$, $\{\hat{f}_k(x_k + \alpha_k d_k)\}$ the resulting stochastic process has desirable convergence properties in expectation.

Inspired by a number of definitions in the model-based literature for stochastic or subsampled methods [3, 18, 29, 32], we introduce a notion of sufficient accuracy for our model function and its derivatives.

Definition 3.1 *Given a realization of Algorithm 1 and an iteration index k , the model $\hat{f}_k : \mathbb{R}^n \mapsto \mathbb{R}$ is said to be $(\delta_f, \delta_g, \delta_H)$ -accurate with respect to (f, x_k, α_k, d_k) when*

$$|f(x_k) - \hat{f}_k(x_k)| \leq \delta_f \quad \text{and} \quad |f(x_k + \alpha_k d_k) - \hat{f}_k(x_k + \alpha_k d_k)| \leq \delta_f, \quad (8)$$

$$\|\nabla f(x_k) - \nabla \hat{f}_k(x_k)\| \leq \delta_g \quad \text{and} \quad \|\nabla f(x_k + \alpha_k d_k) - \nabla \hat{f}_k(x_k + \alpha_k d_k)\| \leq \delta_g, \quad (9)$$

$$\|\nabla^2 f(x_k) - \nabla^2 \hat{f}_k(x_k)\| \leq \delta_H, \quad (10)$$

where $\delta_f, \delta_g, \delta_H$ are nonnegative constants.

Condition (8) is instrumental in establishing decrease guarantees for our method, while conditions (9) and (10) play a key role in defining proper notions of stationarity (see Section 4). Since we are operating with a sequence of random samples and models, we need a probabilistic equivalent of Definition 3.1, which is given below.

Definition 3.2 *Let $p \in (0, 1]$, $\delta_f \geq 0$, $\delta_g \geq 0$ and $\delta_H \geq 0$. A sequence of functions $\{\hat{f}_k\}_k$ is called p -probabilistically $(\delta_f, \delta_g, \delta_H)$ -accurate for Algorithm 1 if the events*

$$I_k := \left\{ \hat{f}_k \text{ is } (\delta_f, \delta_g, \delta_H)\text{-accurate with respect to } (f, x_k, \alpha_k, d_k) \right\} \text{ satisfy } p_k := \mathbb{P}(I_k | \mathcal{F}_{k-1}) \geq p,$$

where \mathcal{F}_{k-1} is the σ -algebra generated by the sample sets $\mathcal{S}_0, \mathcal{S}_1, \dots, \mathcal{S}_{k-1}$, and we define $\mathbb{P}(I_0 | \mathcal{F}_{-1}) := \mathbb{P}(I_0)$.

Observe that if we sample the full data at every iteration (that is, $\mathcal{S}_k = \{1, \dots, N\}$ for all k), the resulting model sequence satisfies the above definition for any $p \in [0, 1]$ and any positive values $\delta_f, \delta_g, \delta_H$. Given our choice of model (2), the accuracy properties are directly related to the random sampling set, but we will follow the existing literature on stochastic optimization

and talk about accuracy of the models. We will however express conditions for good convergence behavior based on the sample size rather than the probability of accuracy.

In the rest of the paper, we assume that the estimate functions of the problem form a probabilistically accurate sequence as follows.

Assumption 3.4 *The sequence $\{\hat{f}_k\}_k$ produced by Algorithm 1 is p -probabilistically δ -accurate, with $\delta := (\delta_f, \delta_g, \delta_H)$ and $p \in (0, 1]$.*

We now introduce the two notions of stationarity that will be considered in our analysis.

Definition 3.3 *Consider a realization of Algorithm 1, and let ϵ_g, ϵ_H be two positive tolerances. We say that the k -th iterate x_k is (ϵ_g, ϵ_H) -model stationary if*

$$\min \{\|g_k\|, \|g(x_{k+1}, \mathcal{S}_k)\|\} \leq \epsilon_g \quad \text{and} \quad \lambda_k \geq -\epsilon_H. \quad (11)$$

Similarly, we will say that x_k is (ϵ_g, ϵ_H) -function stationary if

$$\min \{\|\nabla f(x_k)\|, \|\nabla f(x_{k+1})\|\} \leq \epsilon_g \quad \text{or} \quad \lambda_{\min}(\nabla^2 f(x_k)) \geq -\epsilon_H. \quad (12)$$

Note that the two definitions above are equivalent whenever the model consists of the full function, i.e. when $\mathcal{S}_k = \{1, \dots, n\}$ for all k . We also observe that the definition of model stationarity involves the norm of the vector

$$g_k^+ := g(x_k + \alpha_k d_k; \mathcal{S}_k). \quad (13)$$

The norm of this “next gradient” is a major tool for the derivation of complexity results in Newton-type methods [15, 41]. In a subsampled setting, a distinction between g_k^+ and g_{k+1} is necessary because these two vectors are computed using different samples.

Our objective is to guarantee convergence towards a point satisfying a function stationarity property (12), yet we will only have control on achieving model stationarity. The accuracy of the models will be instrumental in relating the two properties, as shown by the lemma below.

Lemma 3.1 *Let Assumptions 3.1 and 3.2 hold. Consider a realization of the method that reaches an iterate x_k such that x_k is (ϵ_g, ϵ_H) -model stationary. Suppose further that the model \hat{f}_k is $(\delta_f, \delta_g, \delta_H)$ -accurate with*

$$\delta_g \leq \kappa_g \epsilon_g \quad \text{and} \quad \delta_H \leq \kappa_H \epsilon_H \quad (14)$$

where κ_g and κ_H are positive, deterministic constants independent of k . Then, x_k is a $((1 + \kappa_g)\epsilon_g, (1 + \kappa_H)\epsilon_H)$ -function stationary point.

Proof. Proof of Lemma 3.1. Let x_k be an iterate such that $\min\{\|g_k\|, \|g_k^+\|\} \leq \epsilon_g$ and $\lambda_k \geq -\epsilon_H$. Looking at the first property, suppose that $\|g_k\| \leq \epsilon_g$. In that case, we have:

$$\|\nabla f(x_k)\| \leq \|\nabla f(x_k) - g_k\| + \|g_k\| \leq \delta_g + \epsilon_g \leq (\kappa_g + 1)\epsilon_g.$$

A similar reasoning shows that if $\|g_k^+\| \leq \epsilon_g$, we obtain $\|\nabla f(x_{k+1})\| \leq (\kappa_g + 1)\epsilon_g$; thus, we must have

$$\min \{\|\nabla f(x_k)\|, \|\nabla f(x_{k+1})\|\} \leq (1 + \kappa_g)\epsilon_g.$$

Consider now a unit eigenvector v for $\nabla^2 f(x_k)$ associated with $\lambda_{\min}(\nabla^2 f(x_k))$, one has

$$\lambda_k - \lambda_{\min}(\nabla^2 f(x_k)) \leq v^\top H_k v - v^\top \nabla^2 f(x_k) v \leq \|H_k - \nabla^2 f(x_k)\| \|v\|^2 \leq \delta_H.$$

Hence, by using (14), one gets

$$\lambda_{\min}(\nabla^2 f(x_k)) = (\lambda_{\min}(\nabla^2 f(x_k)) - \lambda_k) + \lambda_k \geq -\delta_H - \epsilon_H \geq -(\kappa_H + 1)\epsilon_H.$$

Overall, we have shown that

$$\min \{\|\nabla f(x_k)\|, \|\nabla f(x_{k+1})\|\} \leq (1 + \kappa_g)\epsilon_g \quad \text{and} \quad \lambda_{\min}(\nabla^2 f(x_k)) \geq -(1 + \kappa_H)\epsilon_H,$$

and thus x_k is also a $((1 + \kappa_g)\epsilon_g, (1 + \kappa_H)\epsilon_H)$ -function stationary point. \blacksquare

The reciprocal result of Lemma 3.1, which can be proven in a similar fashion will also be of interest to us.

Lemma 3.2 *Consider a realization of Algorithm 1 and the associated k -th iteration. Suppose that x_k is not $((1 + \kappa_g)\epsilon_g, (1 + \kappa_H)\epsilon_H)$ -function stationary, and that the model \hat{f}_k is $\delta = (\delta_f, \delta_g, \delta_H)$ -accurate with $\delta_g \leq \kappa_g \epsilon_g$ and $\delta_H \leq \kappa_H \epsilon_H$ where κ_g and κ_H are positive constants. Then, x_k is not (ϵ_g, ϵ_H) -model stationary.*

3.2 A general expected decrease result

In this section, we study the guarantees that can be obtained (in expectation) for the various types of direction considered by our method. By doing so, we identify the necessary requirements on our sampling procedure, as well as on our accuracy threshold for the model values.

In what follows, we will make use of the following constants:

$$c_{nc} := \frac{3\theta}{L_H + \eta}, \quad c_n := \min \left\{ \left[\frac{2}{L_H} \right]^{1/2}, \left[\frac{3\theta}{L_H + \eta} \right] \right\}, \quad c_{rn} := \min \left\{ \frac{1}{1 + \sqrt{1 + L_H/2}}, \left[\frac{6\theta}{L_H + \eta} \right] \right\},$$

$$\bar{j}_{nc} := \left[\log_{\theta} \left(\frac{3}{L_H + \eta} \right) \right]_+, \quad \bar{j}_n := \left[\log_{\theta} \left(\sqrt{\frac{3}{L_H + \eta}} \frac{\epsilon^{1/2}}{\sqrt{U_g}} \right) \right]_+, \quad \bar{j}_{rn} := \left[\log_{\theta} \left(\frac{6}{L_H + \eta} \frac{\epsilon}{U_g} \right) \right]_+,$$

where ϵ is the tolerance used in Algorithm 1. Those constants are related to the line-search steps that can be performed at every iteration of Algorithm 1. As long as the current iterate is not an approximate stationary point of the model, we can bound the number of such steps independently of k . To formalize this property, we introduce the following events for any $k \in \mathbb{N}$:

$$E_k^1 := \{\|g_k\| > \epsilon\}, \quad E_k^+ := \{\|g_k^+\| > \epsilon\}, \quad E_k^2 := \{\lambda_k < -\epsilon^{1/2}\}. \quad (15)$$

We also define

$$\mathcal{E}_k^1 := \{\|\nabla f(x_k)\| > (1 + \kappa_g)\epsilon\} \quad \text{and} \quad \mathcal{E}_k^2 := \{\lambda_{\min}(\nabla^2 f(x_k)) < -(1 + \kappa_H)\epsilon^{1/2}\}. \quad (16)$$

By Lemma 3.1 i.e., under the event I_k , it holds that $E_k^1 \cap E_k^2$ imply $\mathcal{E}_k^1 \cap \mathcal{E}_k^2$.

Assuming event $(E_k^1 \cap E_k^+) \cup E_k^2$ occurs, we can provide a lower bound on the step returned by the line-search process. This is the purpose of the following lemma. Its proof mainly relies on arguments from the deterministic case [41] and is provided in the appendix.

Lemma 3.3 *Let Assumptions 3.1 and 3.2 hold for a realization of Algorithm 1. Consider an iteration k such that $(E_k^1 \cap E_k^+) \cup E_k^2$ occurs. Then, the backtracking line search terminates with the step length $\alpha_k = \theta^{j_k}$, with $j_k \leq \bar{j} + 1$ and*

$$\alpha_k \|d_k\| \geq c \epsilon^{1/2}, \quad (17)$$

where $c := \min\{c_{nc}, c_n, c_{rn}\}$ and $\bar{j} := \max\{\bar{j}_{nc}, \bar{j}_n, \bar{j}_{rn}\}$.

Since we are using estimates of the true function and its derivatives, the decrease guaranteed by Lemma 3.3 may not reflect on the true function values. To address this issue, we provide below a deterministic upper bound on the norm of any step computed by our method. The proof is again to be found in the appendix.

Lemma 3.4 *Let Assumption 3.2 hold for a realization of Algorithm 1. Then, for any index k ,*

$$\|d_k\| \leq \max\{U_H, U_g^{1/2}\}. \quad (18)$$

We will now state and prove our main result on expected decrease of our method by combining the results of Lemmas 3.3 and 3.4. To this end, we introduce the following function on $[0, \infty) \times [0, 1]$:

$$\varrho(t, q) := \max \left\{ 0, 1 - \frac{q \frac{\eta t^3}{12}}{2(1-q)U_L} \right\}, \quad \text{where } U_L := U_g \max\{U_H, U_g^{1/2}\} + \frac{L}{2} \max\{U_H^2, U_g\}. \quad (19)$$

With the convention that $\varrho(t, 1) = 0 \forall t \geq 0$, the function ϱ is well-defined with values in $[0, 1]$, and decreasing in its first and second arguments.

We are now ready to establish a guarantee of expected decrease. To this end, define T_ϵ as the first iteration index k of Algorithm 1 for which

$$\min\{\|\nabla f(x_k)\|, \|\nabla f(x_{k+1})\|\} \leq (1 + \kappa_g)\epsilon \quad \text{and} \quad \lambda_{\min}(\nabla^2 f(x_k)) \geq -(1 + \kappa_H)\epsilon^{1/2}.$$

We shall calculate the expected decrease for any iteration k such that $T_\epsilon > k$.

Theorem 3.1 *Let Assumptions 3.1 and 3.2 hold. Suppose also that Assumption 3.4 holds with $\delta = (\delta_f, \delta_g, \delta_H)$ satisfying*

$$\delta_f \leq \frac{\eta}{24} c^3 \epsilon^{3/2}, \quad \delta_g \leq \kappa_g \epsilon, \quad \delta_H \leq \kappa_H \epsilon^{1/2} \quad (20)$$

where $\epsilon > 0$, $\kappa_g \in (0, 1)$, $\kappa_H \in (0, 1)$ and c is chosen as in Lemma 3.3. Then, if the sample fraction π_k is chosen such that

$$\pi_k \geq \varrho(c\epsilon^{1/2}, p), \quad (21)$$

where ϱ is given by (19), then

$$\begin{aligned} & \mathbb{E} [f(x_k + \alpha_k d_k) - f(x_k) \mid \mathcal{F}_{k-1}, \mathcal{E}_k^1 \cup \mathcal{E}_k^2] \\ & \leq -p \frac{\eta c^3}{24} \epsilon^{3/2} \mathbb{P}(E_k^+ \mid \mathcal{F}_{k-1}, E_k^1 \cup E_k^2, I_k) + \min \left\{ 0, \frac{2-p}{1-p} \right\} \frac{\eta c^3}{24} \epsilon^{3/2} \mathbb{P}(\overline{E_k^+} \mid \mathcal{F}_{k-1}, E_k^1 \cup E_k^2, I_k) \end{aligned}$$

Proof. Proof of Theorem 3.1. By definition, one has that:

$$\begin{aligned}
& \mathbb{E} [f(x_{k+1}) - f(x_k) \mid \mathcal{F}_{k-1}, \mathcal{E}_k^1 \cup \mathcal{E}_k^2] \\
&= \tilde{p}_k \mathbb{E} [f(x_{k+1}) - f(x_k) \mid \mathcal{F}_{k-1}, \mathcal{E}_k^1 \cup \mathcal{E}_k^2, I_k] + (1 - \tilde{p}_k) \mathbb{E} [f(x_{k+1}) - f(x_k) \mid \mathcal{F}_{k-1}, \mathcal{E}_k^1 \cup \mathcal{E}_k^2, \overline{I_k}] \\
&= \tilde{p}_k \mathbb{E} [f(x_{k+1}) - f(x_k) \mid \mathcal{F}_{k-1}, E_k^1 \cup E_k^2, I_k] + (1 - \tilde{p}_k) \mathbb{E} [f(x_{k+1}) - f(x_k) \mid \mathcal{F}_{k-1}, \mathcal{E}_k^1 \cup \mathcal{E}_k^2, \overline{I_k}] \quad (23)
\end{aligned}$$

in which I_k is the event corresponding to the model being δ -accurate and $\tilde{p}_k := \mathbb{P}(I_k \mid \mathcal{F}_{k-1}, \mathcal{E}_k^1 \cup \mathcal{E}_k^2)$, and we have used the equivalence of $E_k^1 \cup E_k^2$ and $\mathcal{E}_k^1 \cup \mathcal{E}_k^2$ under I_k . Recall that \mathcal{E}_k^1 and \mathcal{E}_k^2 only depend on the history of the algorithm prior to iteration $k-1$, thus the σ -algebra generated by $\mathcal{E}_k^1 \cup \mathcal{E}_k^2$ is included in \mathcal{F}_{k-1} . We can then apply a result from probability theory [21, Theorem 5.1.6] stating that for any random variable X (not necessarily belonging to \mathcal{F}_{k-1}), we have:

$$\mathbb{E} [X \mid \mathcal{F}_{k-1}, \mathcal{E}_k^1 \cup \mathcal{E}_k^2] = \mathbb{E} [\mathbb{E} [X \mid \mathcal{F}_{k-1}] \mid \mathcal{F}_{k-1}, \mathcal{E}_k^1 \cup \mathcal{E}_k^2] \quad (24)$$

Therefore, denoting by $\mathbf{1}(I_k)$ the indicator variable of the random event I_k , we have

$$\begin{aligned}
\tilde{p}_k = \mathbb{P}(I_k \mid \mathcal{F}_{k-1}, \mathcal{E}_k^1 \cup \mathcal{E}_k^2) &= \mathbb{E} [\mathbf{1}(I_k) \mid \mathcal{F}_{k-1}, \mathcal{E}_k^1 \cup \mathcal{E}_k^2] = \mathbb{E} [\mathbb{E} [\mathbf{1}(I_k) \mid \mathcal{F}_{k-1}] \mid \mathcal{F}_{k-1}, \mathcal{E}_k^1 \cup \mathcal{E}_k^2] \\
&= \mathbb{E} [\mathbb{P}(I_k \mid \mathcal{F}_{k-1}) \mid \mathcal{F}_{k-1}, \mathcal{E}_k^1 \cup \mathcal{E}_k^2] = \mathbb{E} [p_k \mid \mathcal{F}_{k-1}, \mathcal{E}_k^1 \cup \mathcal{E}_k^2] = p_k \geq p,
\end{aligned}$$

where the last equality comes from $p_k \in \mathcal{F}_{k-1}$.

It thus suffices to bound the two terms in (23) independently to bound the expected change in the function values. We begin by the term corresponding to the occurrence of I_k in (23), and use the following decomposition:

$$\begin{aligned}
& \mathbb{E} [f(x_{k+1}) - f(x_k) \mid \mathcal{F}_{k-1}, E_k^1 \cup E_k^2, I_k] \\
&= \mathbb{E} [f(x_{k+1}) - f(x_k) \mid \mathcal{F}_{k-1}, E_k^1 \cup E_k^2, I_k, E_k^+] \mathbb{P}(E_k^+ \mid \mathcal{F}_{k-1}, E_k^1 \cup E_k^2, I_k) \\
&\quad + \mathbb{E} [f(x_{k+1}) - f(x_k) \mid \mathcal{F}_{k-1}, E_k^1 \cup E_k^2, I_k, \overline{E_k^+}] \mathbb{P}(\overline{E_k^+} \mid \mathcal{F}_{k-1}, E_k^1 \cup E_k^2, I_k).
\end{aligned}$$

When the event $E_k^{\text{sta}} = (E_k^1 \cap E_k^+) \cup E_k^2 \cup I_k$ occurs, we can bound the first term of the right hand side as follows:

$$\begin{aligned}
f(x_k + \alpha_k d_k) - f(x_k) &= f(x_k + \alpha_k d_k) - \hat{f}_k(x_k + \alpha_k d_k) + \hat{f}_k(x_k + \alpha_k d_k) - \hat{f}_k(x_k) + \hat{f}_k(x_k) - f(x_k) \\
&\leq 2\delta_f + \hat{f}_k(x_k + \alpha_k d_k) - \hat{f}_k(x_k) \\
&\leq 2\delta_f - \frac{\eta}{6} \alpha_k^3 \|d_k\|^3 \\
&\leq \frac{\eta c^3}{12} \epsilon^{3/2} - \frac{\eta}{6} \alpha_k^3 \|d_k\|^3 \quad (25)
\end{aligned}$$

$$\leq -\frac{\eta}{12} \alpha_k^3 \|d_k\|^3 \leq -\frac{\eta c^3}{12} \epsilon^{3/2}, \quad (26)$$

where (25) comes from the bound (20) on δ_f , and (26) follows from Lemma 3.3.

If we now condition on $E_k^1 \cup E_k^2, I_k$ and consider that E_k^+ does not occur, we can no longer apply Lemma 3.3, but the derivation up to (25) still holds since the method does not stop at iteration k . Overall, we obtain

$$\begin{aligned}
& \mathbb{E} [f(x_{k+1}) - f(x_k) \mid \mathcal{F}_{k-1}, E_k^1 \cup E_k^2, I_k] \\
&\leq -\frac{\eta c^3}{12} \epsilon^{3/2} \mathbb{P}(E_k^+ \mid \mathcal{F}_{k-1}, E_k^1 \cup E_k^2, I_k) + \frac{\eta c^3}{12} \epsilon^{3/2} \mathbb{P}(\overline{E_k^+} \mid \mathcal{F}_{k-1}, E_k^1 \cup E_k^2, I_k). \quad (27)
\end{aligned}$$

We now turn to the second case in (23), for which we exploit the following decomposition:

$$f(x_k + \alpha_k d_k) - f(x_k) = \pi_k \left(\hat{f}_k(x_k + \alpha_k d_k) - \hat{f}_k(x_k) \right) + (1 - \pi_k) \left(f_{\mathcal{S}_k^c}(x_k + \alpha_k d_k) - f_{\mathcal{S}_k^c}(x_k) \right),$$

with $f_{\mathcal{S}_k^c} = \frac{1}{N - |\mathcal{S}_k|} \sum_{i \notin \mathcal{S}_k} f_i$. Using the decrease condition (7) to bound the first term, and a first-order Taylor expansion to bound the second term, we obtain:

$$\begin{aligned} f(x_k + \alpha_k d_k) - f(x_k) &\leq -\pi_k \frac{\eta}{6} \alpha_k^3 \|d_k\|^3 + (1 - \pi_k) \frac{1}{N - |\mathcal{S}_k|} \sum_{i \notin \mathcal{S}_k} \left\{ \alpha_k \nabla f_i(x_k)^\top d_k + \frac{L_i}{2} \alpha_k^2 \|d_k\|^2 \right\} \\ &\leq -\pi_k \frac{\eta}{6} \alpha_k^3 \|d_k\|^3 + (1 - \pi_k) \max_{i \notin \mathcal{S}_k} \left\{ \alpha_k \nabla f_i(x_k)^\top d_k + \frac{L_i}{2} \alpha_k^2 \|d_k\|^2 \right\} \\ &\leq -\pi_k \frac{\eta}{6} \alpha_k^3 \|d_k\|^3 + (1 - \pi_k) \left\{ \alpha_k \|\nabla f_{i_k}(x_k)\| \|d_k\| + \frac{L_{i_k}}{2} \alpha_k^2 \|d_k\|^2 \right\}, \end{aligned}$$

where $i_k \in \arg \max_{i \notin \mathcal{S}_k} \left\{ \alpha_k \nabla f_i(x_k)^\top d_k + \frac{L_i}{2} \alpha_k^2 \|d_k\|^2 \right\}$ and we used the Lipschitz continuity assumption on the functions f_i 's. Introducing the constants U_g and L to remove the dependencies on i_k , we further obtain:

$$f(x_k + \alpha_k d_k) - f(x_k) \leq -\pi_k \frac{\eta}{6} \alpha_k^3 \|d_k\|^3 + (1 - \pi_k) \left\{ U_g \alpha_k \|d_k\| + \frac{L}{2} \alpha_k^2 \|d_k\|^2 \right\}.$$

Using now Lemma 3.4, we arrive at:

$$f(x_k + \alpha_k d_k) - f(x_k) \leq (1 - \pi_k) \left\{ U_g \max\{U_H, U_g^{1/2}\} + \frac{L}{2} \max\{U_H^2, U_g\} \right\} = (1 - \pi_k) U_L,$$

where U_L is defined as in (19), and we use (21) to obtain the last inequality.

Putting all cases together yields:

$$\begin{aligned} &\mathbb{E} [f(x_k + \alpha_k d_k) - f(x_k) | \mathcal{F}_{k-1}, \mathcal{E}_k^1 \cup \mathcal{E}_k^2] \\ &\leq -\tilde{p}_k \frac{\eta c^3}{12} \epsilon^{3/2} \mathbb{P}(E_k^+ | \mathcal{F}_{k-1}, E_k^1 \cup E_k^2, I_k) + \tilde{p}_k \frac{\eta c^3}{12} \epsilon^{3/2} \mathbb{P}(\overline{E_k^+} | \mathcal{F}_{k-1}, E_k^1 \cup E_k^2, I_k) + (1 - \tilde{p}_k) (1 - \pi_k) U_L \\ &= \left[-\tilde{p}_k \frac{\eta c^3}{12} \epsilon^{3/2} + (1 - \tilde{p}_k) (1 - \pi_k) U_L \right] \mathbb{P}(E_k^+ | \mathcal{F}_{k-1}, E_k^1 \cup E_k^2, I_k) \\ &\quad + \tilde{p}_k \frac{\eta c^3}{12} \epsilon^{3/2} \mathbb{P}(\overline{E_k^+} | \mathcal{F}_{k-1}, E_k^1 \cup E_k^2, I_k) + (1 - \tilde{p}_k) (1 - \pi_k) U_L (1 - \mathbb{P}(E_k^+ | \mathcal{F}_{k-1}, E_k^1 \cup E_k^2, I_k)) \\ &\leq \left[-p \frac{\eta c^3}{12} \epsilon^{3/2} + (1 - p) (1 - \pi_k) U_L \right] \mathbb{P}(E_k^+ | \mathcal{F}_{k-1}, E_k^1 \cup E_k^2, I_k) \\ &\quad + \frac{\eta c^3}{12} \epsilon^{3/2} \mathbb{P}(\overline{E_k^+} | \mathcal{F}_{k-1}, E_k^1 \cup E_k^2, I_k) + (1 - \pi_k) U_L (1 - \mathbb{P}(E_k^+ | \mathcal{F}_{k-1}, E_k^1 \cup E_k^2, I_k)) \\ &\leq \left[-p \frac{\eta c^3}{12} \epsilon^{3/2} + (1 - p) (1 - \pi_k) U_L \right] \mathbb{P}(E_k^+ | \mathcal{F}_{k-1}, E_k^1 \cup E_k^2, I_k) \\ &\quad + \left[\frac{\eta c^3}{12} \epsilon^{3/2} + (1 - \pi_k) U_L \right] \mathbb{P}(\overline{E_k^+} | \mathcal{F}_{k-1}, E_k^1 \cup E_k^2, I_k). \end{aligned} \tag{28}$$

Finally, the bound (21) guarantees that

$$1 - \pi_k \leq \frac{p\eta c^3}{24(1-p)U_L} \epsilon^{3/2} \implies \begin{cases} -p\frac{\eta c^3}{12} \epsilon^{3/2} + (1-p)(1-\pi_k)U_L \leq -p\frac{\eta c^3}{24} \epsilon^{3/2}; \\ \frac{\eta c^3}{12} \epsilon^{3/2} + (1-\pi_k)U_L \leq \left(\frac{2-p}{1-p}\right) \frac{\eta c^3}{24} \epsilon^{3/2}. \end{cases}$$

when $\pi_k < 1$ and $p < 1$. Plugging these inequalities into (28) leads to the desired result. The result trivially holds also for $\pi_k = 1$ or $p = 1$.

■

We now comment on the assumptions needed to establish Theorem 3.1. First, we observe that the accuracy requirements (20) can arise as a direct consequence of π_k being sufficiently high (see the online companion for a full illustration). However, it also encompasses the use of inexact values on top of sampling, one particular case being the use of approximate values and derivatives in a deterministic framework (i.e. $\pi_k = 1$ and inexact values are used). Secondly, we point out that the result of Theorem 3.1 is established under a uniform bound on the sampling fraction π_k : although this suggests to use a constant value for π_k (which we do in our experiments), this does not preclude from using an adaptive value for π_k . Indeed, any value satisfying (21) would suit our purpose, thus the choice of π_k could be made adaptively by increasing the sample size. Moreover, the proof of Theorem 3.1 helps in identifying iteration-dependent quantities that could be used as bounds on π_k , e.g. via (28). Still, such (random) quantities are challenging to estimate in practice, and it is unclear whether their manipulation in the upcoming convergence analysis can lead to complexity guarantees such as those presented in the next section: we thus elected to focus on a constant lower bound for the sample size.

4 Global convergence rate and complexity analysis

In this section, we build on Theorem 3.1 to derive a global rate of convergence towards an approximate stationary point in expectation for Algorithm 1. More precisely, we seek an $((1 + \kappa_g)\epsilon, (1 + \kappa_H)\epsilon^{1/2})$ -function stationary point in the sense of Definition 3.3, that is, an iterate satisfying:

$$\min \{ \|\nabla f(x_k)\|, \|\nabla f(x_{k+1})\| \} \leq (1 + \kappa_g)\epsilon \quad \text{and} \quad \lambda_{\min}(\nabla^2 f(x_k)) \geq -(1 + \kappa_H)\epsilon^{1/2}. \quad (29)$$

Since our method only operates with a (subsampling) model of the objective, we are only able to check whether the current iterate is an $(\epsilon, \epsilon^{1/2})$ -model stationary point according to Definition 3.3, i.e. an iterate x_k such that $\min\{\|g_k\|, \|g_k^+\|\} \leq \epsilon$ and $\lambda_k \geq -\epsilon^{1/2}$. Compared to the general setting of Definition 3.3, we are using $\epsilon_g = \epsilon_H^2 = \epsilon$. This specific choice of first- and second-order tolerances has been observed to yield optimal complexity bounds for a number of algorithms, in the sense that the dependence on ϵ is minimal (see e.g. [14, 41]). The rules defining what kind of direction (negative curvature, Newton, etc) is chosen at every iteration of Algorithm 1 implicitly rely on this choice.

Our goal is to relate the model stationarity property (11) to its function stationarity counterpart (29). For this purpose, we first establish a general result regarding the expected number of iterations required to reach function stationarity. We then introduce a stopping criterion involving multiple consecutive iterations of model stationarity: with this criterion, our algorithm can be guaranteed to terminate at a function stationary point with high probability. Moreover, the

expected number of iterations until this termination occurs is of the same order of magnitude as the expected number of iterations required to reach a stationary point.

4.1 Expected iteration complexity

The proof of our expected complexity bound relies upon two arguments from martingales and stopping time theory. The first one is a martingale convergence result [37, Theorem 1], which we adapt to our setting in Theorem 4.1.

Theorem 4.1 *Let $(\Omega, \Sigma, \mathbb{P})$ be a probability space and $\{\Sigma^k\}_k$ be a sequence of sub-sigma algebras of Σ such that $\Sigma^k \subset \Sigma^{k+1}$. If ζ^k is a positively valued sequence of random variables on Σ , and if there exists a deterministic sequence $\nu^k \geq 0$ such that $\mathbb{E}[\zeta^{k+1} | \Sigma^k] + \nu^k \leq \zeta^k$, then ζ^k converges to a $[0, \infty)$ -valued random variable almost surely and $\sum_k \nu^k < \infty$.*

At each iteration, Theorem 3.1 guarantees a certain expected decrease for the objective function. Theorem 4.1 will be used to show that such a decrease cannot hold indefinitely if the objective is bounded from below.

The second argument comes from stopping time analysis (see, e.g., [40, Theorem 6.4.1]) and is given in Theorem 4.2. The notations have been adapted to our setting.

Theorem 4.2 *Let T be a stopping time for the process $\{Z_k, k \geq 0\}$ and let $\bar{Z}_k = Z_k$ for $k \leq T$ and $\bar{Z}_k = Z_T$ for $k > T$. If either one of the three properties hold: (i) \bar{Z}_k is uniformly bounded; (ii) T is bounded; or (iii) $\mathbb{E}[T] < \infty$ and there is an $R < \infty$ such that $\mathbb{E}[|Z_{k+1} - Z_k| | Z_0, \dots, Z_k] < R$. Then, $\mathbb{E}[\bar{Z}_k] \rightarrow \mathbb{E}[Z_T]$.*

Moreover, $\mathbb{E}[Z_T] \geq \mathbb{E}[Z_0]$ (resp. $\mathbb{E}[Z_T] \leq \mathbb{E}[Z_0]$) if $\{Z_k\}$ is a submartingale (resp. a supermartingale).

Theorem 4.2 enables us to exploit the martingale-like property of Definition 3.2 in order to characterize the index of the first stationary point encountered by the method. Using both theorems along with Theorem 3.1, we bound the expected number of iterations needed by Algorithm 1 to produce an approximate function stationary point for the model.

Theorem 4.3 *Let Assumptions 3.1, 3.2 and 3.4 hold, with $\delta = (\delta_f, \delta_g, \delta_H)$ satisfying (20). Suppose that for every index k , the sample size π_k satisfies (21). Denote T_ϵ to be the first iteration index k of Algorithm 1 for which*

$$\min\{\|\nabla f(x_k)\|, \|\nabla f(x_{k+1})\|\} \leq (1 + \kappa_g)\epsilon \quad \text{and} \quad \lambda_{\min}(\nabla^2 f(x_k)) \geq -(1 + \kappa_H)\epsilon^{1/2}.$$

Then, $T_\epsilon < \infty$ almost surely, and

$$\mathbb{E}[T_\epsilon] \leq \frac{(f(x_0) - f_{\text{low}})}{c_\epsilon} + 1, \quad \text{where } c_\epsilon = p\hat{c}\epsilon^{3/2} \quad \text{and} \quad \hat{c} = \frac{\eta}{24}c^3. \quad (30)$$

Proof. Proof of Theorem 4.3. We first observe that both x_{k+1} and the sample size \mathcal{S}_k belong to \mathcal{F}_k , implying that $\{T_\epsilon = k\} \in \mathcal{F}_k$ for all k and T_ϵ is indeed a stopping time.

We first show that the event $\{T_\epsilon = \infty\}$ has a zero probability of occurrence. To this end, we suppose that for every iteration index k , we have $k < T_\epsilon$. Recalling the definitions of $\mathcal{E}_k^1 := \{\|\nabla f(x_k)\| > (1 + \kappa_g)\epsilon\}$ and $\mathcal{E}_k^2 := \{\lambda_{\min}(\nabla^2 f(x_k)) < -(1 + \kappa_H)\epsilon^{1/2}\}$, having $k < T_\epsilon$

implies that the events $(\mathcal{E}_0^1 \cap \mathcal{E}_1^1) \cup \mathcal{E}_0^2, \dots, (\mathcal{E}_k^1 \cap \mathcal{E}_{k+1}^1) \cup \mathcal{E}_k^2$ occur, where we recall that both \mathcal{E}_j^1 and \mathcal{E}_j^2 belong to \mathcal{F}_{j-1} . We thus define the following filtration:

$$\mathcal{T}_0 = \mathcal{F}_{-1} \cap (\mathcal{E}_0^1 \cup \mathcal{E}_0^2), \quad \mathcal{T}_k = \mathcal{F}_{k-1} \cap ((\mathcal{E}_0^1 \cup \mathcal{E}_0^2) \cap \dots \cap (\mathcal{E}_k^1 \cup \mathcal{E}_k^2)) \quad \forall k \geq 1, \quad (31)$$

where we use $\mathcal{F} \cap E$ to denote the trace σ -algebra of the event E on the σ -algebra \mathcal{F} , i.e., $\mathcal{F} \cap E = \{E \cap F : F \in \mathcal{F}\}$. For every $k \geq 0$ and any event A , we thus have $\mathcal{T}_k \subset \mathcal{T}_{k+1}$ and (by the same argument used to establish (24)), we obtain

$$\mathbb{E}[A | \mathcal{T}_k] = \mathbb{E}[\mathbb{E}[A | \mathcal{F}_{k-1}, \mathcal{E}_k^1 \cup \mathcal{E}_k^2] | \mathcal{T}_k].$$

If $T_\epsilon = \infty$, then the assumptions of Theorem 3.1 are satisfied for all iterations k . In particular, for all k , the events \mathcal{E}_k^1 , \mathcal{E}_{k+1}^1 and \mathcal{E}_k^2 occur. Moreover, under the event I_k , \mathcal{E}_k^i and E_k^i , $i = 1, 2$ occur also and are equivalent, hence

$$\mathbb{P}(\overline{E_k^+} | \mathcal{F}_{k-1}, E_k^1 \cup E_k^2, I_k) = 1 - \mathbb{P}(E_k^+ | \mathcal{F}_{k-1}, E_k^1 \cup E_k^2, I_k) = 0$$

Thus, from Theorem 3.1, one gets

$$\mathbb{E}[f(x_k + \alpha_k d_k) - f(x_k) | \mathcal{F}_{k-1}, \mathcal{E}_k^1 \cup \mathcal{E}_k^2] \leq -c_\epsilon.$$

Thus, since $x_k \in \mathcal{T}_k$, we obtain

$$\mathbb{E}[f(x_{k+1}) | \mathcal{T}_k] + c_\epsilon \leq f(x_k),$$

Subtracting f_{low} on both sides, we obtain

$$\mathbb{E}[f(x_{k+1}) - f_{\text{low}} | \mathcal{T}_k] + c_\epsilon \leq f(x_k) - f_{\text{low}}. \quad (32)$$

As a result, we can apply Theorem 4.1 with $\alpha^k = f(x_k) - f_{\text{low}} \geq 0$, $\Sigma^k = \mathcal{T}_k$ and $\nu^k = c_\epsilon > 0$: we thus obtain that $\sum_{k=0}^{\infty} c_\epsilon < \infty$, which is obviously false. This implies that T_ϵ must be finite almost surely.

Consider now the sequence of random variables given by,

$$R_k = f(x_{\min(k, T_\epsilon)}) + \max(\min(k, T_\epsilon) - 1, 0) c_\epsilon.$$

For any $k < T_\epsilon$, we have occurrence of $\mathcal{E}_k^1 \cup \mathcal{E}_k^2$. As in the proof of Theorem 3.1, we use the fact that $(I_k, E_k^1 \cup E_k^2)$ and $(I_k, \mathcal{E}_k^1 \cup \mathcal{E}_k^2)$ have the same logical value for $k < T_\epsilon$, hence $\mathbb{P}(\overline{E_k^+} | \mathcal{F}_{k-1}, E_k^1 \cup E_k^2, I_k, k < T_\epsilon) = 0$. This leads to

$$\mathbb{E}[R_{k+1} | \mathcal{T}_k, k < T_\epsilon] = \mathbb{E}[R_{k+1} | \mathcal{F}_{k-1}, \mathcal{E}_k^1 \cup \mathcal{E}_k^2, k < T_\epsilon] = \mathbb{E}[f(x_{k+1}) | \mathcal{T}_k] + k c_\epsilon \leq f(x_k) - c_\epsilon + k c_\epsilon \leq R_k.$$

Therefore, $\mathbb{E}[R_{k+1} | \mathcal{T}_k, k < T_\epsilon] \leq R_k$ while $R_{k+1} = R_k$ when $k \geq T_\epsilon$, implying that R_k is a supermartingale. Moreover, this supermartingale has bounded expected increments, since

$$\begin{aligned} \mathbb{E}[|R_{k+1} - R_k| | \mathcal{T}_k] &= \mathbb{E}[|f(x_{k+1}) + (k+1)c_\epsilon - f(x_k) - kc_\epsilon| | \mathcal{T}_k] \\ &\leq \mathbb{E}[|f(x_{k+1}) - f(x_k)| + c_\epsilon | \mathcal{T}_k] \leq c_\epsilon + \max(c_\epsilon, f_{\text{max}} - f_{\text{low}}) < \infty \end{aligned}$$

Noting that $T_\epsilon < \infty$ almost surely, we satisfy the assumptions of Theorem 4.2: it thus holds that $\mathbb{E}[R_{T_\epsilon}] \leq \mathbb{E}[R_0]$, leading to

$$f_{\text{low}} + (\mathbb{E}[T_\epsilon] - 1)c_\epsilon \leq \mathbb{E}[R_{T_\epsilon}] \leq \mathbb{E}[R_0] = f(x_0).$$

Re-arranging the terms leads to

$$\mathbb{E}[T_\epsilon] \leq \frac{(f(x_0) - f_{\text{low}})}{c_\epsilon} + 1,$$

which is the desired result. ■

The result of Theorem 4.3 gives a worst-case complexity bound on the expected number of iterations until a function stationarity point is reached. This does not provide a practical stopping criterion for the algorithm, because only *model* stationarity can be tested for during an algorithmic run (even though in the case of $\pi_k = p = 1$, both notions of stationarity are equivalent). Still, by combining Theorem 4.3 and Lemma 3.1, we can show that after at most $\mathcal{O}(p\epsilon^{-3/2})$ iterations on average, if the model is accurate, then the corresponding iterate will be function stationary.

In our algorithm, we assume that accuracy is only guaranteed with a certain probability at every iteration. As a result, stopping after encountering an iterate that is model stationary only comes with a weak guarantee of returning a point that is function stationary. In developing an appropriate stopping criterion, we wish to avoid such “false positives”. To this end, one possibility consists of requiring model stationarity to be satisfied for a certain number of successive iterations. Our approach is motivated by the following result, proved in the online companion.

Proposition 4.1 *Under the assumptions of Theorem 4.3, suppose that Algorithm 1 reaches an iteration index $k + J$ such that for every $j \in \{k, k + 1, \dots, k + J\}$, $\min\{\|g_j\|, \|g_j^+\|\} \leq \epsilon$ and $\lambda_j \geq -\epsilon^{1/2}$. Suppose further that δ_g and δ_H satisfy (14), and that the sample sizes are selected independently of the current iterate. Then, with probability at least $1 - (1 - p)^{J+1}$, where p is the lower bound on p_k given by Assumption 3.4, one of the iterates $\{x_k, x_{k+1}, \dots, x_{k+J}\}$ is $((1 + \kappa_g)\epsilon, (1 + \kappa_H)\epsilon^{1/2})$ -function stationary.*

The result of Proposition 4.1 is only of interest if we can ensure that such a sequence of model stationary iterates can occur in a bounded number of iterations. This will be the case provided we reject iterates for which we cannot certify sufficient decrease, hence the following additional assumption.

Assumption 4.1 *In Algorithm 1, Step 7 is replaced by:*

7'. If $\min\{\|g_k\|, \|g_k^+\|\} < \epsilon$ and $\lambda_k > -\epsilon^{1/2}$, set $x_{k+1} = x_k$, otherwise set $x_{k+1} = x_k + \alpha_k d_k$.

Moreover, the sample size is selected independently of the current iterate so that $\mathbb{P}(I_k | \mathcal{F}_{k-1}) = p$ where p is defined in Assumption 3.4.

This algorithmic change allows us to measure stationarity at a given iterate based on a series of samples. Note that our method now requires two gradient evaluations, but that those involve the same sample. Under a slightly stronger set of assumptions, Proposition 4.2 then guarantees that sequences of model stationary points of arbitrary length will occur in expectation. The proof of this result can be found in the online companion.

Proposition 4.2 *Let Assumptions 3.1, 3.2, 3.4 and 4.1 hold, where δ satisfies (20) with $\kappa_g, \kappa_H \in (0, 1)$, and $p_k = p \forall k$. For a given $J \in \mathbb{N}$, define $T_{\epsilon, J}^m$ as the first iteration index of Algorithm 1 for which*

$$\min\{\|g_k\|, \|g_k^+\|\} < \epsilon \quad \text{and} \quad \lambda_k > -\epsilon^{1/2}, \quad \forall k \in \{T_{\epsilon, J}^m, T_{\epsilon, J}^m + 1, \dots, T_{\epsilon, J}^m + J\}. \quad (33)$$

Suppose finally that for every index k , the sample size π_k satisfies

$$\forall k, \quad \pi_k \geq \varrho(c\hat{\epsilon}^{1/2}, p), \quad (34)$$

where $\hat{\epsilon} = \min\{\frac{1-\kappa_g}{1+\kappa_g}, \frac{(1-\kappa_H)^2}{(1+\kappa_H)^2}\}\epsilon$. (Note that $\varrho(c\hat{\epsilon}^{1/2}, p) \geq \varrho(c\epsilon^{1/2}, p)$.)

Then, $T_{\epsilon, J}^m < \infty$ almost surely, and

$$\mathbb{E}[T_{\epsilon, J}^m] \leq \frac{(f(x_0) - f_{\text{low}})}{c_{\hat{\epsilon}}} + J + 1 \quad \text{where } c_{\hat{\epsilon}} = p\hat{c}\hat{\epsilon}^{3/2} \quad \text{and} \quad \hat{c} = \frac{\eta}{24}c^3. \quad (35)$$

With the result of Proposition 4.2, we are guaranteed that there will exist consecutive iterations satisfying model stationarity in expectation. Checking for stationarity over successive iterations thus represents a valid stopping criterion in practice. If an estimate of the probability p is known, one can even choose J to guarantee that the probability of computing a stationary iterate is sufficiently high.

To end this section, we establish a bound in expectation on the number of evaluations of f_i needed to reach a stationary point. Note that we must account for the additional objective evaluations induced by the line-search process (see [41, Theorem 8] for details).

Corollary 4.1 *Let Assumptions 3.1, 3.2, 3.4 and 4.1 hold, where δ satisfies (20) with $\kappa_g, \kappa_H \in (0, 1)$, and $p_k = p$ for every k . Suppose also that $\pi_k \geq \varrho(c\hat{\epsilon}^{1/2}, p)$, then the expected number of evaluations of ∇f_i and $\nabla^2 f_i$ are respectively bounded above by*

$$\frac{3(f(x_0) - f_{\text{low}})}{p\hat{c}}\epsilon^{-3/2} + 1 \quad (36)$$

while the expected number of function evaluations is bounded above by

$$(1 + \max\{j_{nc}, j_n, j_{rn}\})p^{-(J+1)} \left[\frac{(f(x_0) - f_{\text{low}})}{p\hat{c}}\hat{\epsilon}^{-3/2} + J + 1 \right].$$

4.2 Sample and evaluation complexity for uniform sampling

4.2.1 Comparison with the deterministic line-search method:

In general, we can consider that at each iteration we must perform $|\mathcal{S}_k|n$ computations to evaluate the sample gradient, $|\mathcal{S}_k|n^2$ to compute the sample Hessian, and evaluate a function $\bar{j}|\mathcal{S}_k|$ times during the line search. Per Lemma 3.3, the maximum number of line-search iterations \bar{j} can be considered of the order $\log(1/\epsilon)$. As a result, each iteration requires $|\mathcal{S}_k|(n + n^2 + \log(1/\epsilon))$ computations. For our sampling rate to yield improvement over the deterministic (fully sampled) method, we require $N \log(1/\epsilon)$ to be much larger than $|\mathcal{S}_k|n^2$, implying that the appropriate regime for this algorithm is one where the number of variables is considerably less than the number of data points.

To illustrate the theoretical results, we now comment on the two main requirements made in the analysis of the Section 4 are related to the function value accuracy δ_f and the sample size π_k . More precisely, for a given tolerance ϵ , we required in Theorem 4.3 that:

1. $\delta_f \leq \frac{\eta}{24} c^3 \epsilon^{3/2}$, $\delta_g \leq \kappa_g \epsilon$, $\delta_H \leq \kappa_H \epsilon^{1/2}$.
2. $\pi_k \geq \varrho(c\epsilon^{1/2}, p)$.

In this section, we provide estimates of the minimum number of samples necessary to achieve those two conditions in the case of a uniform sampling strategy. To facilitate the exposure, we discard the case $p = 1$, for which the properties above trivially hold, and focus on $p \in (0, 1)$. Although we focus on the properties required for Theorem 4.3, note that a similar analysis holds for the requirements of Proposition 4.2.

For the rest of the section, we suppose that the set \mathcal{S}_k is formed of $n\bar{\pi}$ indexes chosen uniformly at random with replacement. where $\bar{\pi}$ is independent of k . That is, for every $i \in \mathcal{S}_k$ and every $j = 1, \dots, N$, we have $\mathbb{P}(i = j) = \frac{1}{N}$. This case has been well studied in the case of subsampled Hessian [46] and subsampled gradient [39]. The next theorem derives the result regarding the required conditions on π_n to ensure the event I_k . The theorem uses standard arguments (e.g., [46, Lemma 16] and [38, Lemma 2]); for completeness, its proof is given in the appendix.

Theorem 4.4 *Let Assumptions 1 and 2 hold. For any $p \in (0, 1)$, let $\hat{p} = \frac{p+3}{4}$. Suppose that the sample fractions π_k of Algorithm 1 are chosen to satisfy $\pi_k \geq \pi(\epsilon)$ for every k , where*

$$\pi(\epsilon) := \frac{1}{N} \max \left\{ N \varrho(c\epsilon^{1/2}, \hat{p}), \frac{9216 f_{\text{up}}^2}{\eta^2 c^6 \epsilon^3} \ln \left(\frac{2}{1-\hat{p}} \right), \frac{U_g^2}{\kappa_g^2 \epsilon^2} \left[1 + \sqrt{8 \ln \left(\frac{1}{1-\hat{p}} \right)} \right]^2, \frac{16L^2}{\kappa_H^2 \epsilon} \ln \left(\frac{2N}{1-\hat{p}} \right) \right\}.$$

Then, the model sequence is p -probabilistically $(\delta_f, \delta_g, \delta_H)$ -accurate with $\delta_f = \frac{\eta}{24} c^3 \epsilon^{3/2}$, $\delta_g = \kappa_g \epsilon$ and $\delta_H = \kappa_H \epsilon^{1/2}$. Moreover, all the results from Section 4.1 hold.

We observe that explicit computation of these bounds would require estimating L, L_H, U_H , and U_g . If the orders of magnitude for the aforementioned quantities are available, they can be used for choosing the sample size. In addition, note that the bound presented is global, i.e., it should hold for every iterate k , however, it is also possible to consider these problem constants as they hold over a region, and thus when x_k is in this region π_k can be potentially adjusted accordingly in an adaptive fashion, if some local estimates for these constants could be made available.

4.2.2 Comparison with other sample complexities:

By comparing it with sample complexity results available in the literature, we can position our method within the existing landscape of results, and get insight about the cost of second-order requirements, as well as that of using inexact function values.

When applied to nonconvex problems, a standard stochastic gradient approach with fixed step size has a complexity in $\mathcal{O}(\epsilon^{-4})$ (both in terms of iterations and gradient evaluations) for reaching approximate first-order optimality [23]. Modified SGD methods that take curvature information can significantly improve over that bound, and even possess second-order guarantees.

Typical guarantees are provided in terms of function stationarity (though this condition cannot be checked in practice), and hold with high probability. Our results hold in expectation, but involve a model stationary condition that we can check at every iteration. Moreover, it is

possible to convert a rate in expectation into high-probability rates (of same order), following for instance an argument used for trust-region algorithms with probabilistic models [24].

It is also interesting to compare our complexity orders with those obtained by first-order methods in stochastic optimization. Stochastic trust-region methods [18, 29] require $\mathcal{O}(\Delta_k^{-4})$ samples per iteration, where Δ_k is the trust-region radius and serves as an approximation of the norm of the gradient. The line-search algorithm of [35] guarantees sufficient accuracy in the function values if the sample size is of order $\mathcal{O}(\alpha_k^{-2}\|g_k\|^{-4})$ (we use our notations for consistency). By comparison our method requires $\mathcal{O}(\epsilon^{-3/2})$ samples, where $\epsilon^{-3/2}$ is used as a proxy for $\alpha_k^{-3}\|d_k\|^3$. Our sample complexity can thus be higher than that of other methods, in that it does not depend on the iteration level. On the other hand, this makes our approach well-defined, and enables the derivation of second-order guarantees, while previously proposed methods such as that of Paquette and Scheinberg [35] is only concerned with first-order guarantees.

Finally, we discuss sample bounds for Newton-based methods in a subsampling context. In [46], it was shown that the desired complexity rate of $\mathcal{O}(\epsilon^{-3/2})$ is achieved with probability $1 - p$, if for every k , the sample size (for approximating the Hessian) satisfies:

$$|\mathcal{S}_k| \geq \frac{16U_H^2}{\epsilon} \ln\left(\frac{2N}{p}\right)$$

The same result is used in [32]. In both cases, the sample sizes are inversely proportional to the desired tolerance squared. In [49], high probability results were derived with the accuracy of the function gradient and Hessian estimates δ_g and δ_H being bounded by ϵ and $\epsilon^{1/2}$, respectively. The resulting sampling bounds are $\mathcal{O}(\epsilon^{-2})$. In our setting, we additionally require the function accuracy to be of order $\epsilon^{3/2}$, where ϵ is the gradient tolerance, yet the other dependencies on ϵ in terms of gradient and Hessian sampling matches previous bounds in the case of exact function values and subsampled derivatives [46, 49]. In that sense, we can identify the cost induced by assuming that only inexact function values are available.

Finally, we observe that our sample size requirements are proportional to n^2 , while the upper bound U_g on the gradients can also grow with n . Thus, unless the setting is a regime with a very large number of data samples and a relatively small number of variables, the computed required sampling size could approach N . It appears that this is an issue associated with the required worst-case sampling rates for higher-order sampling algorithms in general, given the literature described above. To the best of our knowledge, tightening these bounds in a general setting remains an open area of research, even though improved sample complexities can be obtained by exploiting various specific problem structures. Though out of the scope of this work, we remark that practical approaches use less samples to approximate second-order information than they use to approximate first-order information [13].

5 Numerical experiments

In this section, we present a numerical study of an implementation of our proposed framework on several machine learning tasks involving both real and simulated data. Our goal is to advocate for the use of second-order methods, such as the one described in this paper, for certain training problems with a nonconvex optimization landscape. We are particularly interested in highlighting notable advantages of going beyond first-order algorithms, which are still the preferred approaches in most machine learning problems. Indeed, first-order methods have lower computational complexity than second-order methods (that is, they require less work to compute a step

at each iteration), but second-order methods possess better iteration complexity than first-order ones (they converge in fewer iterations). In many machine learning settings, lower computational complexity trumps iteration complexity, and therefore first-order algorithms are viewed as superior. Nevertheless, our results suggest that second-order schemes can be competitive in certain contexts.

We focus our experiments on architectures with a relatively small number of network parameters (optimization variables). We point out that there exist important problems where the number of optimization variables n is indeed small compared to the number of samples N . Besides logistic regression and shallow networks, the recent interest in formulating sparser architectures such as `efficientnet` [42] for problems training huge amounts of data, in order to lighten memory loads in computation-heavy and memory-light HPC hardware, indicates the potential for increased applications of this sort in the future.

Although the most popular variants of SGD in practice such as `ADAM` [26] incorporate advanced features, we believe that there is value in putting our approach in perspective with a simple framework emblematic of the first-order methods used in machine learning. For these reasons, we compare our implementation with a vanilla SGD method using a constant step size (learning rate). We place ourselves in a setting in which the learning rate is tuned among a set of predefined values corresponding to standard choices. Our goal is to highlight the sensitivity of such a method to this hyperparameter, and to compare it with our scheme for a given batch size.

5.1 Implementation

We first describe the modifications to Algorithm 1 that we made in the implementation (which we identify as `ALAS` in this section). Algorithm 1 differed from the method of [41] in that we did not consider steps along the negative gradient direction, in order to simplify our theoretical analysis. We have re-introduced these steps in our implementation. This change for practical performance has proper intuitive justification: if the negative gradient direction is already a good direction of negative curvature, or the Hessian is flat along its direction, then the negative gradient direction already enjoys second-order properties that ensure it is a good descent direction for the function. In our experiments, these steps can be taken, but the vast majority of steps correspond to cases in Algorithm 1 (see Figure 1 and the online companion for an illustration of this behavior). Secondly, we modified the condition to select a negative curvature step from $\lambda_k < -\epsilon^{1/2}$ to $\lambda_k < -\|g_k\|^{1/2}$. The former was necessary to handle the case of a stationary point for which $\|g_k^+\| < \epsilon \leq \|g_k\|$ and $\lambda_k > -\epsilon^{1/2}$ in an appropriate fashion in the analysis of Section 3 in the main text, but this case was rarely encountered in practice. Thirdly, we replaced the cubic decrease condition by a sufficient decrease quadratic in the norm of the step. This is again for performance reasons, and although theoretical results could be established using this condition, it does not appear possible to obtain the same dependencies in ϵ as given in Theorem 4. We recall that the cubic decrease condition has been instrumental in deriving optimal iteration complexity bounds for Newton-type methods [15, 41]. The detailed description of `ALAS` as implemented is provided in the appendix.

In our implementation of `ALAS`, we chose the values $\epsilon = 10^{-5}$, $\eta = 10^{-2}$, and $\theta = 0.9$. The `ALAS` framework and a standard stochastic gradient descent (SGD) algorithm were both implemented in Python 3.7. For fair comparison, we compare the performance of `ALAS` and `SGD` using the same batch size, or percentage of the dataset taken as samples in each iteration (p_k

in the theory). Various Python libraries were used, including JAX [12] for efficient compilation and automatic differentiation, as well as NumPy [45], SciPy [25] and Pandas [34]. The smallest eigenvalue λ_k and the negative curvature step are computed using the “scipy.sparse.linalg.eigs” routine. All our experiments were run using Intel Xeon CPU at 2.30 GHz and 25.51 GB of RAM, using a Linux distribution Ubuntu 18.04.3 LTS with Linux kernel 4.14.137.

5.2 Classification on the IJCNN1 dataset

We first tested our algorithms on a binary classification task for the IJCNN1 dataset (with $N = 49,990$ samples and $n = 22$ features per sample). Our goal was to train a neural network for binary classification. We used two different architectures: one had one hidden layer with 4 neurons, the other had two hidden layers with 4 neurons each. Both networks used the hyperbolic tangent activation function $\phi(x) = \frac{\exp(2x)-1}{\exp(2x)+1}$ and mean-squared error (MSE) loss, resulting in a twice continuously differentiable optimization problem, with a highly nonlinear objective. The results we present were obtained using samples corresponding to 20 %, 10 %, 5% and 1% of the dataset, with a runtime of 10 seconds. The dataset was partitioned into disjoint samples of given sizes for each data pass (epoch) and these samples were randomly repartitioned every data pass. The MSE loss is defined as

$$l(\mathcal{B}) = \frac{1}{|\mathcal{B}|} \sum_{i \in \mathcal{B}} (y_i - \hat{y}_i)^2, \quad (37)$$

where \mathcal{B} is the sampled dataset (mini-batch), $|\mathcal{B}|$ the size of the mini-batch, $y_i \in \{-1, 1\}$ the actual binary label of the sample i and \hat{y}_i is the predicted label of for the sample i .

We tested SGD with several possible values for the learning rate, namely 1, 0.6, 0.3, 0.1, 0.01, 0.001 (the details are available in the online companion), and selected the best variant for comparison with ALAS. Note that the step size in ALAS is selected adaptively through a line search, which makes this method more robust. Figure 3 shows the noise and robustness of the performance by reporting the median and 90% level confidence interval for the trajectory over 200 runs for each batch size. Note that ALAS is fairly consistent, while the precision and variability of SGD can change in a complex way depending on the learning rate. Figure 4 plots the training accuracy associated with the trajectories and their variation, which match what we observed on the loss plots.

Figures 5 and 6 compare ALAS and SGD with the classical learning rate value for this task (0.01) on the two networks with one and two hidden layers, respectively. The results are summarized in Table 1, where we compare ALAS with the best SGD variant and the standard variant with a learning rate of 0.01. To mitigate the iteration and overall cost of both algorithms, we compared the methods based on the minimal error reached over the last 10 seconds of the run and on the median loss over the last two seconds. In all the tables, the scalar in the parenthesis for SGD entries is the learning rate and the column *median loss [8-10]s* shows the median loss over the last two seconds. In general, ALAS outperforms SGD on the IJCNN1 task in terms of these metrics. Another interesting observation is the performance of ALAS appears to be fairly stable as its trajectory appears monotonic: in fact, the trajectory can exhibit non-monotonic trends (see Section 5.3 and the online companion), but those are less prominent than for the SGD method. Our interpretation is that the “bad case” of poor estimates yielding an inaccurate noisy step and more poor estimates resulting in its acceptance is fairly uncommon in the stochastic setting because our model provides a high-order stochastic estimate of the

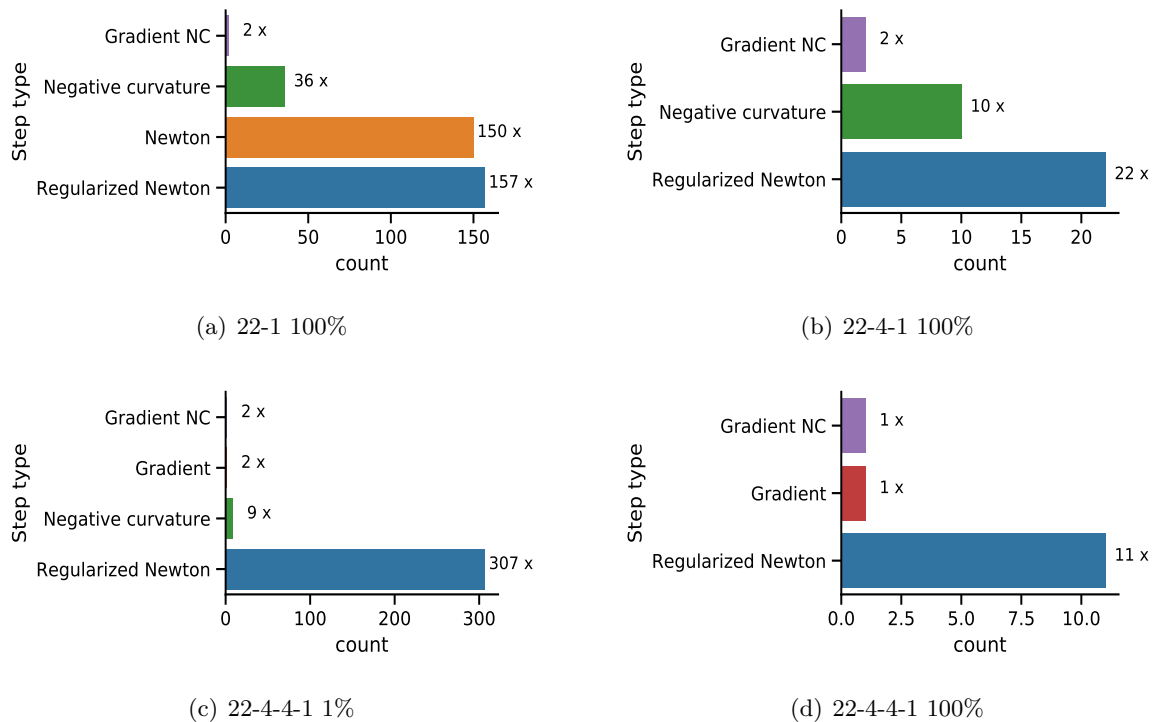


Figure 1: The step type distribution of a single run of ALAS algorithm on the IJCNN1 task for different architectures and sampling sizes.

function. On the contrary, SGD can easily yield ascent in the loss function if the gradient samples correspond to components that are far from their mean, i.e. the true gradient.

We further study the behavior of ALAS by first looking at the types of steps taken by the method on selected runs for the IJCNN1 task, shown in Figure 1. This distribution is highly dependent of the network architecture but some common patterns were observed. The most frequent type of step is *Regularized Newton*, but other steps (in particular, along stochastic gradient directions, which we added in our implementation) occur in a small percentage of cases. Note that negative curvature directions are computed, highlighting the nonconvex nature of our problem. In addition, we illustrate typical numbers of line-search iterations for our problem in Figure 2: in general, this number is relatively mild, but the line-search process may require a significant number of function evaluations. Given that a worst-case example of this behavior is Figure 2(b) where all samples are used, we attribute this to the architecture rather than to the line-search process itself.

5.3 Transfer learning using MNIST

The current implementation of ALAS is very suitable for transfer learning, where only a few layers of a neural network need to be trained (i.e. only a few parameters need to be optimized). To demonstrate this, we first trained all the parameters in a convolutional neural network (CNN) on a subset of the MNIST dataset [30] (classification of digits 0 - 7). The CNN had 9 convolution layers (with 16 filters for the first layer, 32 filters for the second one, 64 filters for

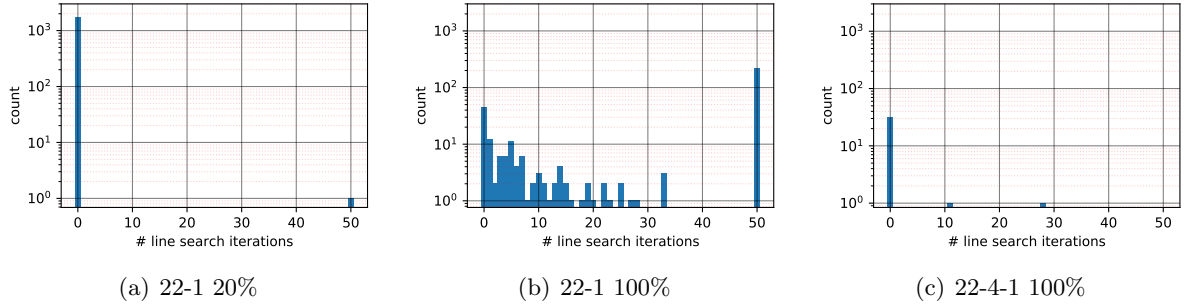


Figure 2: Plots of the number of line-search iterations during each update for the IJCNN1 task for selected runs of the ALAS algorithm with different architectures and sampling sizes. The maximum number of line-search iterations was set to 50.

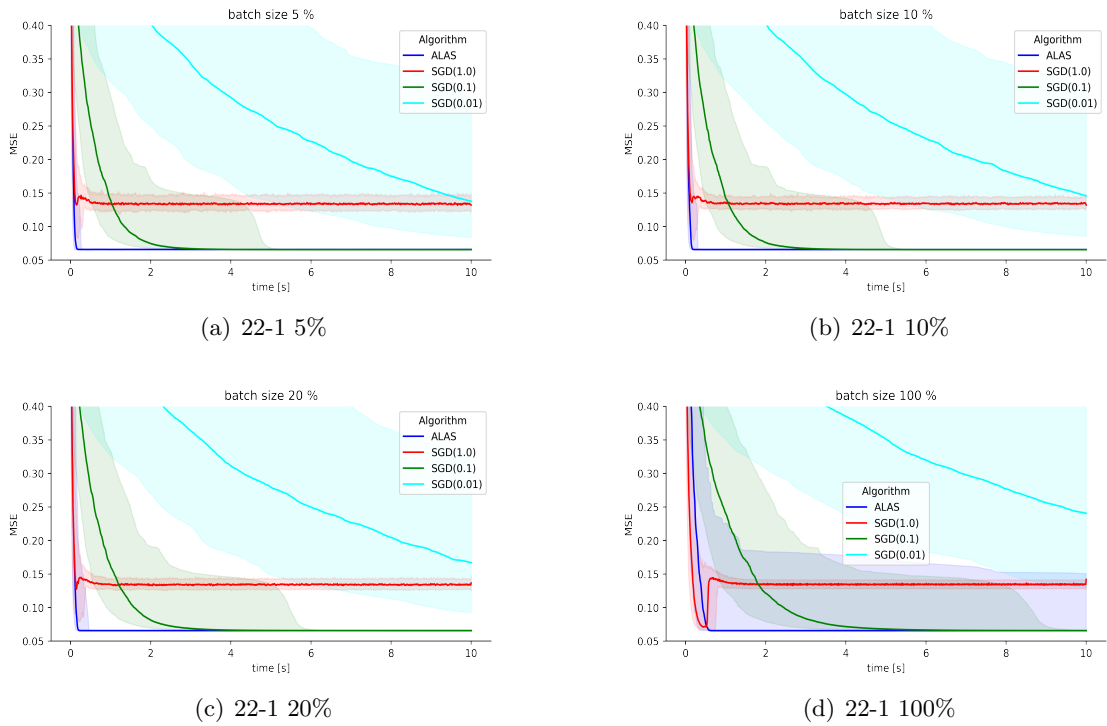


Figure 3: Comparison of ALAS and SGD (with a default learning rate 0.01) on the IJCNN1 dataset with a simple neural network with 22 input neurons, reporting the median and 95% confidence interval across 200 runs

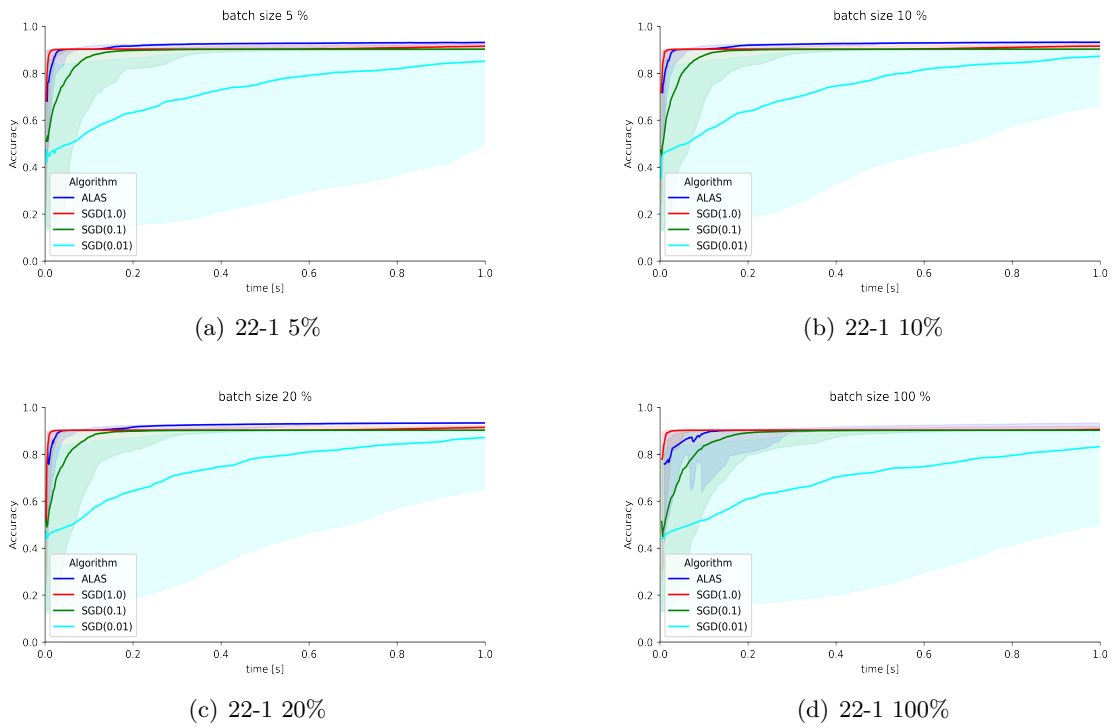


Figure 4: Comparison of levels of training accuracy for the training achieved by ALAS and SGD (with a default learning rate 0.01) on the IJCNN1 dataset with a simple neural network with 22 input neurons, reporting the median and 95% confidence interval across 200 runs

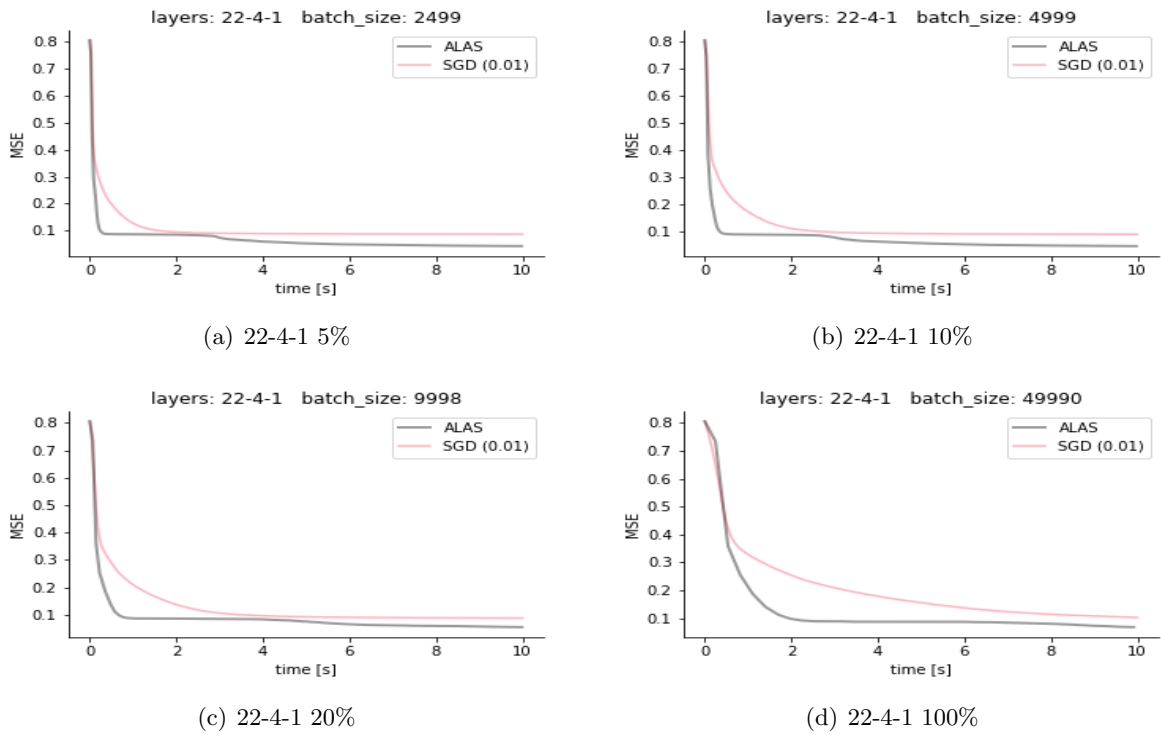


Figure 5: Comparison of ALAS and SGD (with a default learning rate 0.01) on the IJCNN1 dataset with a simple neural network with 22 input neurons, 4 neurons in the hidden layer and an output neuron.

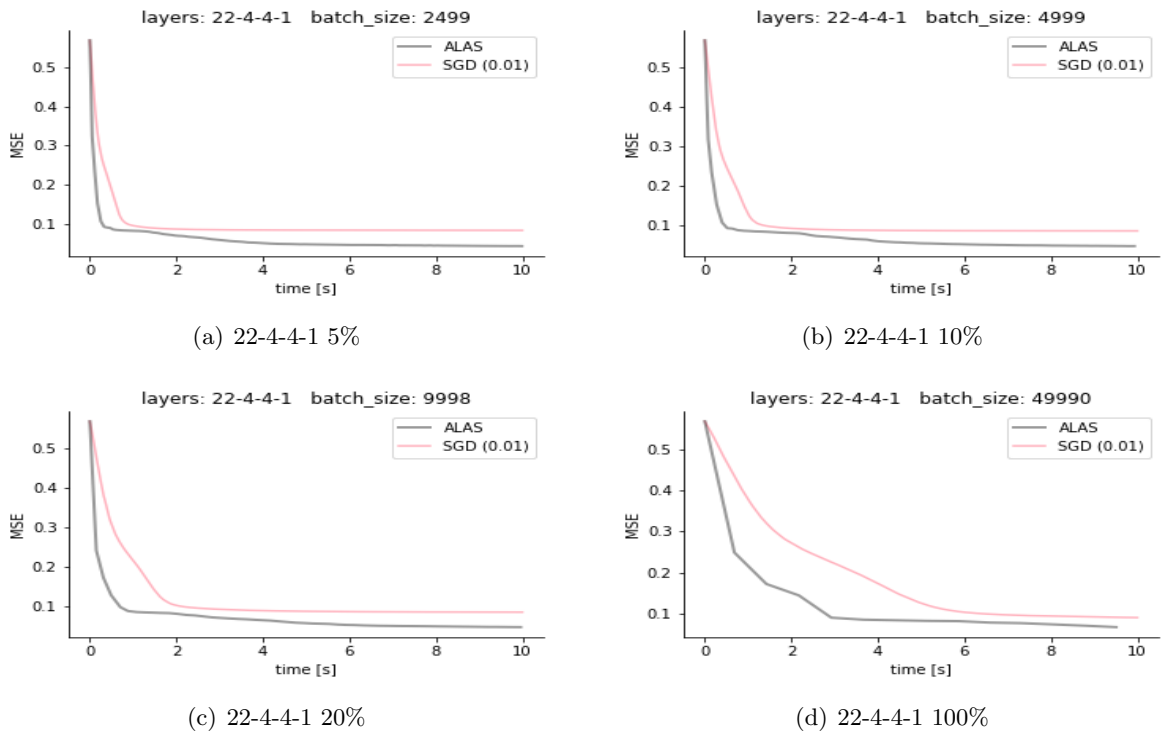


Figure 6: Comparison of ALAS and SGD (with a default learning rate 0.01) on the IJCNN1 dataset with a simple neural network with 22 input neurons, two hidden layers each with 4 neurons and an output neuron.

Layers: 22-4-1					Layers: 22-4-4-1				
alg.	π_k	min loss	loss [8-10]s	iter.	alg.	π_k	min loss	loss [8-10]s	iter.
ALAS	1%	0.0463	0.0478	551	ALAS	1%	0.0434	0.0451	320
SGD (0.3)	1%	0.0528	0.0558	12033	SGD (0.3)	1%	0.0438	0.0454	11121
SGD (0.01)	1%	0.0872	0.0873	11779	SGD (0.01)	1%	0.0841	0.0842	10997
ALAS	5%	0.0449	0.0462	238	ALAS	5%	0.0450	0.0457	114
SGD (0.6)	5%	0.0514	0.0569	8439	SGD (0.3)	5%	0.0468	0.0500	7894
SGD (0.01)	5%	0.0875	0.0876	8471	SGD (0.01)	5%	0.0845	0.0846	7792
ALAS	10%	0.0492	0.0510	124	ALAS	10%	0.0470	0.0477	68
SGD (0.6)	10%	0.0557	0.0626	6293	SGD (0.3)	10%	0.0519	0.0571	5165
SGD (0.01)	10%	0.0880	0.0883	5773	SGD (0.01)	10%	0.0849	0.0850	5191
ALAS	20%	0.0611	0.0628	76	ALAS	20%	0.0491	0.0498	42
SGD (0.6)	20%	0.0598	0.0654	4389	SGD (0.3)	20%	0.0545	0.0587	3728
SGD (0.01)	20%	0.0887	0.0891	4443	SGD (0.01)	20%	0.0852	0.0854	3694

Table 1: Results over the time period $t = 10$ s on the IJCNN1 task.

the other layers), followed by a global max pooling layer and a single dense classification layer with softmax activation function and 25% dropout for the eight digits (8 output neurons). Once this network was trained, the classification layer was removed and the extracted features were used for transfer learning to classify the remaining two digits (8 and 9) images of the MNIST dataset, that were unseen during the training of the original CNN. The new classification layers were then trained using the ALAS and the SGD algorithms (we did the tests using the following step sizes 1, 0.6, 0.3, 0.1), with sample sizes corresponding to 100%, 20 %, 10 %, and 5% of the entire data. The total number of samples with the digits 8 and 9 is $N = 11800$ and the input to the trained layer are 8 neurons. The optimized function was the MSE. As shown in Table 2, ALAS outperformed the SGD variants in most of the runs. Note that when the whole dataset was used, i.e. $\mathcal{S}_k = \{1, \dots, N\}$ for all k , ALAS outperforms the SGD variants by a significant margin for all four neural network architectures.

5.3.1 Transfer learning without pre-computed features

The experiment above is using pre-computed features, i.e. the original images were run through the pre-trained network once and the saved output was used for the optimization of the top layers. While this technique brings massive speed-ups as it is not necessary to compute the outputs for the same images repeatedly, it can only be used when there are repeated images. This prevents the use of online data augmentation, where the individual images are randomly transformed (e.g. rotations, scaling) for each batch and the output from the pre-trained layers has to be recomputed every time.

This is a very favorable scenario for the ALAS algorithm as it usually needs much less updates than the SGD even though each update is more costly in terms of operations — the need to recompute the features every time adds fixed costs to update steps of both SGD and ALAS. We have run the same experiment as above but without the pre-computed features with the time limit 1 hour instead of 10 seconds and with different weight initialization; the results are shown in Table 3 and in Fig 7. Figures 7(c) and 7(d) shows details of the run depicted in Figure 7(b). The number of iterations was similar for both algorithms (only small differences possibly caused by the different utilization of the cloud server) as the feature evaluation step

Layers: 8-1					Layers: 8-1-1				
alg.	π_k	min loss	loss [8-10]s	iter.	alg.	π_k	min loss	loss [8-10]s	iter.
ALAS	5%	0.2739	0.2752	12220	ALAS	5%	0.2721	0.2815	11887
SGD (1.0)	5%	0.2796	0.2801	20264	SGD (0.3)	5%	0.2796	0.2801	20264
ALAS	10%	0.2732	0.2740	11514	ALAS	10%	0.2667	0.2722	10116
SGD (1.0)	10%	0.2795	0.2799	20872	SGD (0.6)	10%	0.2738	0.2753	20649
ALAS	20%	0.2728	0.2732	10691	ALAS	20%	0.2657	0.2704	8593
SGD (1.0)	20%	0.2796	0.2800	20141	SGD (0.6)	20%	0.2736	0.2749	20327
ALAS	100%	0.2587	0.2592	5118	ALAS	100%	0.2362	0.2363	3630
SGD (1.0)	100%	0.2800	0.2803	17832	SGD (0.3)	100%	0.2751	0.2754	16697
Layers: 8-2-1					Layers: 8-4-1				
ALAS	5%	0.2649	0.2762	6964	ALAS	5%	0.2516	0.2567	2245
SGD (1.0)	5%	0.2667	0.2702	20975	SGD (1.0)	5%	0.2524	0.2550	1356
ALAS	10%	0.2632	0.2674	5778	ALAS	10%	0.2524	0.2550	1356
SGD (1.0)	10%	0.2681	0.2705	19502	SGD (1.0)	10%	0.2505	0.2554	19502
ALAS	20%	0.2602	0.2625	3609	ALAS	20%	0.2529	0.2542	811
SGD (1.0)	20%	0.2695	0.2712	16311	SGD (1.0)	20%	0.2504	0.2555	16211
ALAS	100%	0.2295	0.2301	1151	ALAS	100%	0.2227	0.2247	220
SGD (1.0)	100%	0.2754	0.2762	7232	SGD (1.0)	100%	0.2615	0.2645	6377

Table 2: Results reached over the given time period $t = 10$ s on the transfer learning task.

was the dominant for the same $8-4-1$ layer configuration for all sample sizes. For higher number of weights, the ALAS performs comparably less iterations than the SGD as the update step is no longer negligible compared to the feature evaluation using the fixed weight neural network (but that is still quite costly and thus we do not observe order of magnitude differences here) as can be seen in the networks with configurations $8-16-4-1$ (only ALAS was run to show the small drop in number of iterations) and $8-32-16-1$ (the SGD still performs similar number of iterations as for the $8-4-1$ layer configuration).

Layers: 8-4-1					Layers: 8-16-4-1				
alg.	π_k	min loss	loss [3400-3600]s	iter.	alg.	π_k	min loss	loss [3400-3600]s	iter.
ALAS	10%	0.1805	0.2483	1629	ALAS	20 %	0.1884	0.2294	748
SGD (1.0)	10%	0.2003	0.2706	1709	SGD (1.0)	100%	0.2255	0.2680	870
SGD (0.1)	10%	0.2144	0.2853	1683	SGD (0.1)	100%	0.2326	0.2796	869
SGD (0.01)	10%	0.2417	0.3159	1674	SGD (0.01)	100%	0.2517	0.3028	878
ALAS	20%	0.2034	0.2443	871	ALAS	20 %	0.2076	0.2664	562
SGD (1.0)	20%	0.2356	0.2802	878	SGD (0.1)	20%	0.2230	0.2709	887
SGD (0.1)	20%	0.2488	0.2913	848	SGD (0.01)	20%	0.2480	0.2932	876
SGD (0.01)	20%	0.3657	0.3946	900	SGD (1.0)	20%	0.3015	1.9834	886

Table 3: Results reached over the given time period $t = 3600$ s on the transfer learning task.

6 Conclusion

In this paper, we presented a line-search method for stochastic optimization, wherein the Hessian, gradient, and function values must be estimated through subsampling and cannot be obtained

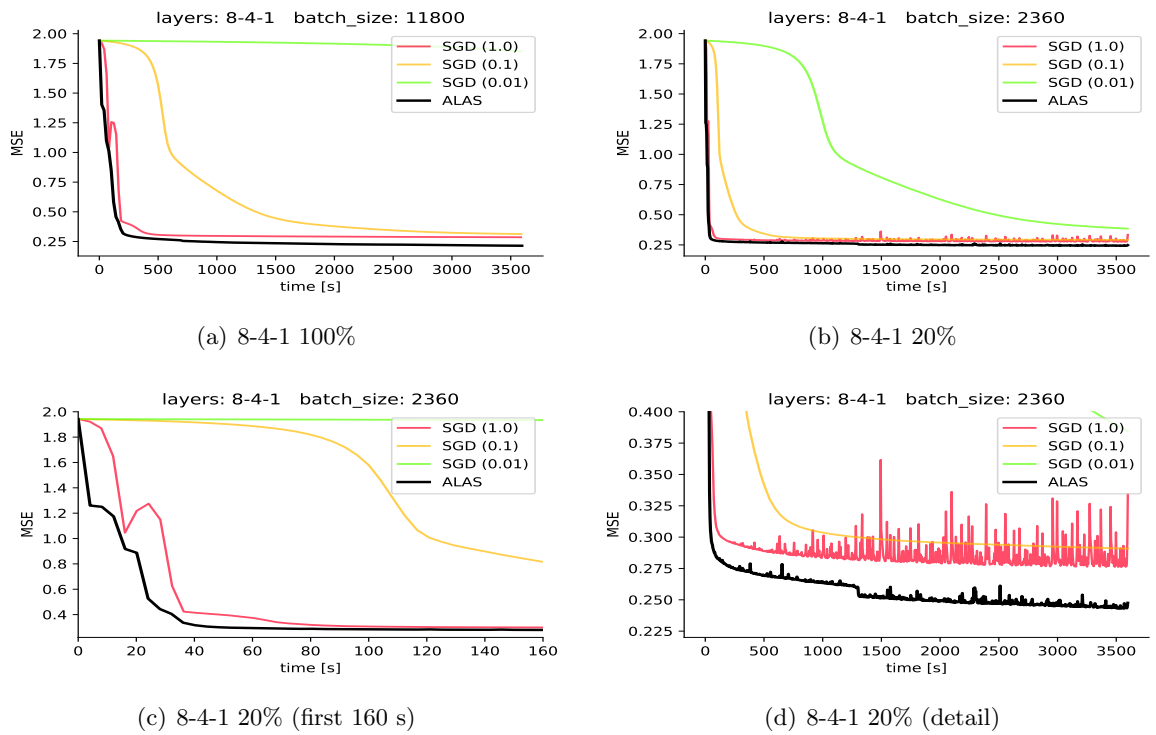


Figure 7: Comparison of ALAS and SGD (with various learning rates) on the transfer learning task without pre-computed features with a simple neural network with 8 input neurons, 4 hidden neurons and an output neuron.

exactly. Using probabilistically accurate models, we derived a complexity result on the expected number of iterations until an approximate measure of stationarity is reached for the current model. This result in expectation is complementary to those holding with high probability, i.e. with probability of drawing an accurate sample at every iteration. We also proposed a practical strategy to assess whether the current iterate is close to a sample point for the original objective, that does not require the computation of the full function. Our numerical experiments showed the potential of the proposed approach on several machine learning tasks, including transfer learning.

We believe that the results of this paper encourage further study of second-order algorithms despite the prevailing paradigm of using first-order methods for their computationally cheap iterations. In particular, our approach could be helpful in generalizing other line-search techniques to the context of subsampled function values while our theoretical analysis, that captures the worst-case behavior of the problem, can likely be refined to exploit the problem structure. Finally, a high-performance implementation of our method would benefit from more practical features such as matrix-free operations and iterative linear algebra (see preliminary numerical results in [28]) as well as adaptive sampling batch sizes, following the recent trends in stochastic optimization [4]. A number of difficulties arise in extending our complexity analysis to these frameworks, yet developing practical schemes with such guarantees is an important and exciting perspective for future research.

Acknowledgments

We are indebted to Courtney Paquette and Katya Scheinberg for raising an issue with the first version of this paper, that lead to significant improvement of its results. We would also like to thank the reviewers of this paper for their insightful comments.

References

- [1] Naman Agarwal, Zeyuan Allen-Zhu, Brian Bullins, Elad Hazan, and Tengyu Ma. Finding approximate local minima faster than gradient descent. In *Annual ACM SIGACT Symposium on Theory of Computing*, pages 1195–1199, 2017.
- [2] Zeyuan Allen-Zhu. Natasha 2: Faster non-convex optimization than SGD. In *Advances in Neural Information Processing Systems*, 2018.
- [3] Afonso S. Bandeira, Katya Scheinberg, and Luis N. Vicente. Convergence of trust-region methods based on probabilistic models. *SIAM J. Optim.*, 24:1238–1264, 2014.
- [4] Stefania Bellavia and Gianmarco Gurioli. Stochastic analysis of an adaptive cubic regularization method under inexact gradient evaluations and dynamic hessian accuracy. *Optimization*, pages 1–35, 2021.
- [5] Albert S. Berahas, Raghu Bollapragada, and Jorge Nocedal. An investigation of Newton-sketch and subsampled Newton methods. *arXiv preprint arXiv:1705.06211*, 2017.
- [6] El Houcine Bergou, Youssef Diouane, Vyacheslav Kungurtsev, and Clément W. Royer. A stochastic Levenberg-Marquardt method using random models with application to data assimilation. *arXiv preprint arXiv:1807.2176*, 2018.

- [7] El Houcine Bergou, Serge Gratton, and Luis N. Vicente. Levenberg-Marquardt methods based on probabilistic gradient models and inexact subproblem solution, with application to data assimilation. *SIAM/ASA J. Uncertain. Quantif.*, 4:924–951, 2016.
- [8] Jose Blanchet, Coralia Cartis, Matt Menickelly, and Katya Scheinberg. Convergence rate analysis of a stochastic trust region method for nonconvex optimization. *INFORMS Journal on Optimization*, 1:92–119, 2019.
- [9] Raghu Bollapragada, Richard H. Byrd, and Jorge Nocedal. Exact and inexact subsampled Newton methods in optimization. *IMA J. Numer. Anal.*, 39:545–578, 2019.
- [10] Raghu Bollapragada, Dheevatsa Mudigere, Jorge Nocedal, Hao-Jun Michael Shi, and Ping Tak Peter Tang. A progressive batching L-BFGS method for machine learning. In *International Conference on Machine Learning*, pages 620–629, 2018.
- [11] Léon Bottou, Frank E. Curtis, and Jorge Nocedal. Optimization methods for large-scale machine learning. *SIAM Rev.*, 60:223–311, 2018.
- [12] James Bradbury, Roy Frostig, Peter Hawkins, Matthew James Johnson, Chris Leary, Dougal Maclaurin, and Skye Wanderman-Milne. *JAX: composable transformations of Python+NumPy programs*, 2018.
- [13] Richard H. Byrd, Gillian M. Chin, Will Neveitt, and Jorge Nocedal. On the use of stochastic Hessian information in optimization methods for machine learning. *SIAM J. Optim.*, 21:977–995, 2011.
- [14] Yair Carmon, John C. Duchi, Oliver Hinder, and Aaron Sidford. Accelerated methods for non-convex optimization. *SIAM J. Optim.*, 28:1751–1772, 2018.
- [15] Coralia Cartis, Nicholas I. M. Gould, and Philippe L. Toint. Adaptive cubic regularisation methods for unconstrained optimization. Part II: worst-case function- and derivative-evaluation complexity. *Math. Program.*, 130:295–319, 2011.
- [16] Coralia Cartis and Katya Scheinberg. Global convergence rate analysis of unconstrained optimization methods based on probabilistic models. *Math. Program.*, 169:337–375, 2018.
- [17] Chih-Chung Chang and Chih-Jen Lin. LIBSVM. *ACM Transactions on Intelligent Systems and Technology*, 2(3):1–27, April 2011.
- [18] Ruobing Chen, Matt Menickelly, and Katya Scheinberg. Stochastic optimization using a trust-region method and random models. *Math. Program.*, 169:447–487, 2018.
- [19] Frank E. Curtis, Katya Scheinberg, and Rui Shi. A stochastic trust-region algorithm based on careful step normalization. *INFORMS Journal on Optimization*, 1:200–220, 2019.
- [20] Yann N. Dauphin, Razvan Pascanu, Caglar Gulcehre, Kyunghyun Cho, Surya Ganguli, and Yoshua Bengio. Identifying and attacking the saddle point problem in high-dimensional non-convex optimization. In *Advances in Neural Information Processing Systems*, pages 2933–2941, 2014.

- [21] Rick Durrett. *Probability: Theory and Examples*. Camb. Ser. Stat. Prob. Math. Cambridge University Press, Cambridge, fourth edition, 2010.
- [22] Murat A Erdogdu and Andrea Montanari. Convergence rates of sub-sampled Newton methods. In *Advances in Neural Information Processing Systems*, pages 3052–3060, 2015.
- [23] Saeed Ghadimi and Guanghui Lan. Stochastic first- and zeroth-order methods for nonconvex stochastic programming. *SIAM J. Optim.*, 23:2341–2368, 2013.
- [24] Serge Gratton, Clément W. Royer, Luis N. Vicente, and Zaikun Zhang. Complexity and global rates of trust-region methods based on probabilistic models. *IMA J. Numer. Anal.*, 38:1579–1597, 2018.
- [25] Eric Jones, Travis Oliphant, Pearu Peterson, et al. SciPy: Open source scientific tools for Python, 2001–. [Online; accessed 2015-05-12].
- [26] Diederik P. Kingma and Jimmy Ba. Adam: A method for stochastic optimization. In *International Conference on Learning Representations*, 2014.
- [27] Jonas Moritz Kohler and Aurélien Lucchi. Sub-sampled cubic regularization for non-convex optimization. In *International Conference on Machine Learning*, pages 1895–1904, 2017.
- [28] Vyacheslav Kungurtsev and Tomas Pevny. Algorithms for solving optimization problems arising from deep neural net models: smooth problems. *Cisco-CTU WP5 Technical Report*, 2016. Originally proprietary industrial report. Currently available online at <https://arxiv.org/abs/1807.00172>.
- [29] Jeffrey Larson and Stephen C. Billups. Stochastic derivative-free optimization using a trust region framework. *Comput. Optim. Appl.*, 64:619–645, 2016.
- [30] Yann LeCun, Corinna Cortes, and Christopher J.C. Burges. MNIST handwritten digit database. *ATT Labs [Online]*. Available: <http://yann.lecun.com/exdb/mnist>, 2, 2010.
- [31] Jason D. Lee, Ioannis Panageas, Georgios Piliouras, Max Simchowitz, Michael I. Jordan, and Benjamin Recht. First-order methods almost always avoid saddle points. *Math. Program.*, 176:311–337, 2019.
- [32] Mingrui Liu and Tianbao Yang. On noisy negative curvature descent: Competing with gradient descent for faster non-convex optimization. *arXiv preprint arXiv:1709.08571*, 2017.
- [33] Maren Mahsereci and Philipp Hennig. Probabilistic line searches for stochastic optimization. *J. Mach. Learn. Res.*, 18:1–59, 2017.
- [34] Wes McKinney. Data structures for statistical computing in python. In Stéfan van der Walt and Jarrod Millman, editors, *Proceedings of the 9th Python in Science Conference*, pages 51 – 56, 2010.
- [35] Courtney Paquette and Katya Scheinberg. A stochastic line search method with convergence rate analysis. *arXiv preprint arXiv:1807.07994*, 2018.
- [36] Mert Pilanci and Martin J. Wainwright. Newton sketch: A linear-time optimization algorithm with linear-quadratic convergence. *SIAM J. Optim.*, 27:205–245, 2017.

- [37] Herbert Robbins and David Siegmund. A convergence theorem for non negative almost supermartingales and some applications. In *Optimizing methods in statistics*, pages 233–257. Elsevier, 1971.
- [38] Farbod Roosta-Khorasani and Michael W. Mahoney. Sub-sampled Newton methods I: Globally convergent algorithms. *arXiv preprint arXiv:1601.04737*, 2016.
- [39] Farbod Roosta-Khorasani and Michael W. Mahoney. Sub-sampled Newton methods. *Math. Program.*, 174:293–326, 2019.
- [40] Sheldon M. Ross. *Stochastic processes*. Wiley, New York, 1996.
- [41] Clément W. Royer and Stephen J. Wright. Complexity analysis of second-order line-search algorithms for smooth nonconvex optimization. *SIAM J. Optim.*, 28:1448–1477, 2018.
- [42] Mingxing Tan and Quoc V. Le. Efficientnet: Rethinking model scaling for convolutional neural networks. *arXiv preprint arXiv:1905.11946*, 2019.
- [43] Nilesh Tripuraneni, Mitchell Stern, Chi Jin, Jeffrey Regier, and Michael I. Jordan. Stochastic cubic regularization for fast nonconvex optimization. In *Advances in Neural Information Processing Systems*, 2018.
- [44] Joel A. Tropp. An introduction to matrix concentration inequalities. *Foundations and Trends in Machine Learning*, 8:1–230, 2015.
- [45] Stefan van der Walt, S. Chris Colbert, and Gaël Varoquaux. The NumPy array: A structure for efficient numerical computation. *Computing in Science & Engineering*, 13(2):22–30, 3 2011.
- [46] Peng Xu, Farbod Roosta-Khorasani, and Michael W. Mahoney. Newton-type methods for non-convex optimization under inexact hessian information. *Math. Program.*, 2019.
- [47] Peng Xu, Jiyan Yang, Farbod Roosta-Khorasani, Christopher Ré, and Michael W. Mahoney. Sub-sampled Newton methods with non-uniform sampling. In *Advances in Neural Information Processing Systems*, 2016.
- [48] Yi Xu, Rong Jin, and Tianbao Yang. First-order stochastic algorithms for escaping from saddle points in almost linear time. In *Advances in Neural Information Processing Systems*, 2018.
- [49] Zhewei Yao, Peng Xu, Farbod Roosta-Khorasani, and Michael W. Mahoney. Inexact non-convex Newton-type methods. *arXiv preprint arXiv:1802.06925*, 2018.

A Supplementary proofs

A.1 Proof of Lemma 3.3

We consider in turn the three possible steps that can be taken at iteration k , and obtain a lower bound on the amount $\alpha_k \|d_k\|$ for each of those.

Case 1: $\lambda_k < -\epsilon^{1/2}$ (negative curvature step). In that case, we apply the same reasoning than in [41, Proof of Lemma 1] with the model \hat{f}_k playing the role of the objective, the backtracking line search terminates with the step length $\alpha_k = \theta^{j_k}$, with $j_k \leq \bar{j}_{nc} + 1$ and $\alpha_k \geq \frac{3\theta}{L_H + \eta}$. When d_k is computed as a negative curvature direction, one has $\|d_k\| = -\lambda_k > 0$. Hence,

$$\alpha_k \|d_k\| \geq \frac{3\theta}{L_H + \eta} [-\lambda_k] = c_{nc} [-\lambda_k] \geq c\epsilon^{1/2}.$$

Case 2: $\lambda_k > \|g_k\|^{1/2}$ (Newton step). Because the stationarity is not achieved and $\lambda_k > 0$ in this case, we necessarily have $\|\tilde{g}_k\| = \min\{\|g_k\|, \|g_k^+\|\} > \epsilon$. From Algorithm 1, we know that d_k is chosen as the Newton step. Hence, using the argument of [41, Proof of Lemma 3] with $\epsilon_H = \epsilon^{1/2}$, the backtracking line search terminates with the step length $\alpha_k = \theta^{j_k}$, where

$$j_k \leq \left\lceil \log_{\theta} \left(\sqrt{\frac{3}{L_H + \eta}} \frac{\epsilon^{1/2}}{\sqrt{U_g}} \right) \right\rceil_+ + 1 = \bar{j}_n + 1,$$

thus the first part of the result holds. If the unit step size is chosen, we have by [41, Relation (23)] that

$$\alpha_k \|d_k\| = \|d_k\| \geq \left[\frac{2}{L_H} \right]^{1/2} \|g(x_k + \alpha_k d_k; \mathcal{S}_k)\|^{1/2} \geq c\epsilon^{1/2}. \quad (38)$$

Consider now the case $\alpha_k < 1$. Using [41, Relations (25) and (26), p. 1457], we have:

$$\begin{aligned} \|d_k\| &\geq \frac{3}{L_H + \eta} \epsilon_H = \frac{3}{L_H + \eta} \epsilon^{1/2} \text{ and} \\ \alpha_k &\geq \theta \sqrt{\frac{3}{L_H + \eta}} \epsilon_H^{1/2} \|d_k\|^{-1/2} = \theta \sqrt{\frac{3}{L_H + \eta}} \epsilon^{1/4} \|d_k\|^{-1/2}. \end{aligned}$$

As a result,

$$\alpha_k \|d_k\| \geq \theta \left[\frac{3}{L_H + \eta} \right]^{1/2} \epsilon^{1/4} \|d_k\|^{-1/2} \|d_k\| \geq \left[\frac{3\theta}{L_H + \eta} \right] \epsilon^{1/2} \geq c\epsilon^{1/2}. \quad (39)$$

Case 3: (Regularized Newton step) This case occurs when the conditions for the other two cases fail, that is, when $-\epsilon^{1/2} \leq \lambda_k \leq \|g_k\|^{1/2}$. We again exploit the fact that the stationarity is not achieved to deduce that we necessarily have $\|\tilde{g}_k\| = \min\{\|g_k\|, \|g_k^+\|\} > \epsilon$. This in turn implies that $\min\{\|\tilde{g}_k\| \epsilon^{-1/2}, \epsilon^{1/2}\} \geq \epsilon^{1/2}$. As in the proof of the previous lemma, we apply the theory of [41, Proof of Lemma 4] using $\epsilon_H = \epsilon^{1/2}$. We then know that the backtracking line search terminates with the step length $\alpha_k = \theta^{j_k}$, with

$$j_k \leq \left\lceil \log_{\theta} \left(\frac{6}{L_H + \eta} \frac{\epsilon}{U_g} \right) \right\rceil_+ + 1 = \bar{j}_{rn} + 1.$$

We now distinguish between the cases $\alpha_k = 1$ and $\alpha_k < 1$. If the unit step size is chosen, we can use [41, relations 30 and 31], where $\nabla f(x_k + d_k)$ and ϵ_H are replaced by g_k^+ and $\epsilon^{1/2}$, respectively. This gives

$$\alpha_k \|d_k\| = \|d_k\| \geq \frac{1}{1 + \sqrt{1 + L_H/2}} \min \left\{ \|g_k^+\| / \epsilon^{1/2}, \epsilon^{1/2} \right\}.$$

Therefore, if the unit step is accepted, one has by [41, equation 31]

$$\alpha_k \|d_k\| \geq \frac{1}{1 + \sqrt{1 + L_H/2}} \min \left\{ \|\tilde{g}_k\| \epsilon^{-1/2}, \epsilon^{1/2} \right\}. \quad (40)$$

Considering the case $\alpha_k < 1$ and using [41, equation 32, p. 1459], we have:

$$\alpha_k \geq \theta \frac{6}{L_H + \eta} \epsilon_H \|d_k\|^{-1} = \frac{6\theta}{L_H + \eta} \epsilon^{1/2} \|d_k\|^{-1},$$

which leads to

$$\alpha_k \|d_k\| \geq \frac{6\theta}{L_H + \eta} \epsilon^{1/2}. \quad (41)$$

Putting (40) and (41) together, we obtain

$$\alpha_k \|d_k\| \geq \min \left\{ \frac{1}{(1 + \sqrt{1 + L_H/2})^3}, \left[\frac{6\theta}{L_H + \eta} \right]^3 \right\} \min \{ \|\tilde{g}_k\| \epsilon^{-1/2}, \epsilon^{1/2} \} = c_{rn} \min \{ \|\tilde{g}_k\| \epsilon^{-1/2}, \epsilon^{1/2} \} \geq c \epsilon^{1/2}.$$

By putting the three cases together, we arrive at the desired conclusion.

A.2 Proof of Lemma 3.4

Indeed, since the lemma trivially holds if $\|d_k\| = 0$, we only need to prove that it holds for $\|d_k\| > 0$. We consider three disjoint cases:

Case 1: $\lambda_k < -\epsilon^{1/2}$. Then the negative curvature step is taken and $\|d_k\| = |\lambda_k| \leq U_H$.

Case 2: $\lambda_k > \|g_k\|^{1/2}$. We can suppose that $\|g_k\| > 0$ because otherwise $\|d_k\| = 0$. Then, d_k is a Newton step with

$$\|d_k\| \leq \|H_k^{-1}\| \|g_k\| \leq \|g_k\|^{-1/2} \|g_k\| \leq \|g_k\|^{1/2} \leq U_g^{1/2}.$$

Case 3: $-\epsilon^{1/2} \leq \lambda_k \leq \|g_k\|^{1/2}$. As in Case 2, we suppose that $\|g_k\| > 0$ as $\|d_k\| = 0$ if this does not hold. Then, d_k is a regularized Newton step with

$$\|d_k\| = \|(H_k + (\|g_k\|^{1/2} + \epsilon^{1/2})\mathbb{I}_n)^{-1} g_k\| \leq \frac{\|g_k\|}{\lambda_k + \|g_k\|^{1/2} + \epsilon^{1/2}} \leq \|g_k\|^{1/2} \leq U_g^{1/2}.$$

where the last inequality uses $\lambda_k + \epsilon^{1/2} \geq 0$ and $\|g_k\| > 0$.

A.3 Proof of Theorem 4.3

To prove Theorem 4.3, we will combine the following three standard lemmas.

Lemma A.1 *Under Assumption 2, consider an iterate x_k of Algorithm 1. For any $p \in (0, 1)$, if the sample set \mathcal{S}_k is chosen to be of size*

$$\bar{\pi} \geq \frac{1}{N} \frac{16L^2}{\delta_H^2} \ln \left(\frac{2N}{1-p} \right), \quad (42)$$

then

$$\mathbb{P} \left(\|H(x_k; \mathcal{S}_k) - \nabla^2 f(x_k)\| \leq \delta_H | \mathcal{F}_{k-1} \right) \geq p.$$

Proof. Proof of Lemma A.1. See [46, Lemma 16]; note that here we are using L_i (Lipschitz constant of ∇f_i) as a bound on $\|\nabla^2 f_i(x_k)\|$, and that we are providing a bound on the sampling fraction $\bar{\pi} = \frac{|\mathcal{S}_k|}{N}$. See also [44, Theorem 1.1], considering the norm as related to the maximum singular vector. ■

By the same reasoning as for Lemma A.1, but in one dimension, we can readily provide a sample size bound for obtaining accurate function values. To this end, we define

$$f_{\text{up}} \geq \max_k \max_{i=1,\dots,N} f_i(x_k). \quad (43)$$

Note that such a bound necessarily exists when the iterates are contained in a compact set. Specific structure of the problem can also guarantee such a bound, even though it may exhibit dependencies on the problem's dimension. For instance, in the case of classification and logistic regression, one has $f_{\text{up}} = 1$, while in the case of (general) regression, one has $f_{\text{up}} \leq C_1 + C_2 \|x\|^2 = \mathcal{O}(n)$. We emphasize that both of these bounds can be very pessimistic.

Lemma A.2 *Under Assumption 3.1, consider an iterate x_k of Algorithm 1. For any $p \in (0, 1)$, if the sample set \mathcal{S}_k is chosen to be of size*

$$\bar{\pi} \geq \frac{1}{N} \frac{16f_{\text{up}}^2}{\delta_f^2} \ln\left(\frac{2}{1-p}\right), \quad (44)$$

then

$$\mathbb{P}\left(\left|\hat{f}(x_k; \mathcal{S}_k) - f(x_k)\right| \leq \delta_f \mid \mathcal{F}_{k-1}\right) \geq p.$$

Proof. Proof of Lemma A.2. The proof follows that of [46, Lemma 4.1] by considering $\hat{f}(x_k; \mathcal{S}_k)$ and $f(x_k)$ as one-dimensional matrices. ■

Lemma A.3 *Under Assumption 3.2, consider an iterate x_k of Algorithm 1. For any $p \in (0, 1)$, if the sample set \mathcal{S}_k is chosen to be of size*

$$\bar{\pi} \geq \frac{1}{N} \frac{U_g^2}{\delta_g^2} \left[1 + \sqrt{8 \ln\left(\frac{1}{1-p}\right)}\right]^2, \quad (45)$$

then

$$\mathbb{P}(\|g(x_k; \mathcal{S}_k) - \nabla f(x_k)\| \leq \delta_g \mid \mathcal{F}_{k-1}) \geq p.$$

Proof. Proof of Lemma A.3. See [38, Lemma 2]. ■

We now combine the three previous lemmas to obtain an overall result indicating the required $\bar{\pi}$ such that Lemmas A.1, A.2 and A.3 simultaneously hold, i.e., the event I_k holds.

Indeed, let $\delta_f = \frac{\eta}{24} c^3 \epsilon^{3/2}$, $\delta_g = \kappa_g \epsilon$, $\delta_H = \kappa_H \epsilon^{1/2}$ and note that,

$$I_k \equiv I_k^h \cap I_k^g \cap I_k^f,$$

where

$$\begin{aligned} I_k^h &:= \{\|H(x_k; \mathcal{S}_k) - \nabla^2 f(x_k)\| \leq \delta_H\} \\ I_k^g &:= \{\|g(x_k; \mathcal{S}_k) - \nabla f(x_k)\| \leq \delta_g\} \\ I_k^f &:= \{|\hat{f}(x_k; \mathcal{S}_k) - f(x_k)| \leq \delta_f\}. \end{aligned}$$

Using the required conditions on π_n , Lemmas [A.1](#), [A.2](#) and [A.3](#) imply

$$\mathbb{P}\left((I_k^f)^c \mid \mathcal{F}_{k-1}\right) \leq 1 - \hat{p}, \quad \mathbb{P}\left((I_k^g)^c \mid \mathcal{F}_{k-1}\right) \leq 1 - \hat{p}, \quad \text{and} \quad \mathbb{P}\left((I_k^h)^c \mid \mathcal{F}_{k-1}\right) \leq 1 - \hat{p}.$$

In the other hand, one has

$$\begin{aligned} \mathbb{P}\left((I_k)^c \mid \mathcal{F}_{k-1}\right) &= \mathbb{P}\left((I_k^f)^c \mid \mathcal{F}_{k-1}\right) + \mathbb{P}\left((I_k^g)^c \mid \mathcal{F}_{k-1}\right) + \mathbb{P}\left((I_k^h)^c \mid \mathcal{F}_{k-1}\right) - \mathbb{P}\left((I_k^f)^c \cap (I_k^g)^c \mid \mathcal{F}_{k-1}\right) \\ &\quad - \mathbb{P}\left((I_k^g)^c \cap (I_k^h)^c \mid \mathcal{F}_{k-1}\right) - \mathbb{P}\left((I_k^f)^c \cap (I_k^h)^c \mid \mathcal{F}_{k-1}\right) + \mathbb{P}\left((I_k^f)^c \cap (I_k^g)^c \cap (I_k^h)^c \mid \mathcal{F}_{k-1}\right) \\ &\leq \mathbb{P}\left((I_k^f)^c \mid \mathcal{F}_{k-1}\right) + \mathbb{P}\left((I_k^g)^c \mid \mathcal{F}_{k-1}\right) + \mathbb{P}\left((I_k^h)^c \mid \mathcal{F}_{k-1}\right) \\ &\quad + \mathbb{P}\left((I_k^f)^c \mid (I_k^h)^c, (I_k^g)^c, \mathcal{F}_{k-1}\right) \mathbb{P}\left((I_k^h)^c \mid (I_k^g)^c, \mathcal{F}_{k-1}\right) \mathbb{P}\left((I_k^g)^c \mid \mathcal{F}_{k-1}\right) \\ &\leq \mathbb{P}\left((I_k^f)^c \mid \mathcal{F}_{k-1}\right) + 2\mathbb{P}\left((I_k^g)^c \mid \mathcal{F}_{k-1}\right) + \mathbb{P}\left((I_k^h)^c \mid \mathcal{F}_{k-1}\right) \leq 4(1 - \hat{p}). \end{aligned}$$

Hence,

$$\mathbb{P}(I_k \mid \mathcal{F}_{k-1}) \geq 1 - 4(1 - \hat{p}) = p,$$

meaning that the model sequence is p -probabilistically $(\delta_f, \delta_g, \delta_H)$ -accurate, thus results from [Section 4.1](#) hold. \square

A.4 Proof of [Proposition 4.1](#)

In this proof, we will use the notation $\mathbb{P}_k(\dots) = \mathbb{P}(\cdot \mid \mathcal{F}_{k-1})$, as well as the random events

$$E = \left\{ \text{One of the iterates in } \{x_{k+j}\}_{j=0..J} \text{ is } ((1 + \kappa_g)\epsilon, (1 + \kappa_H)\epsilon^{1/2})\text{-function stationary} \right\},$$

$$E_j = \left\{ \text{The iterate } x_{k+j} \text{ is } (\epsilon, \epsilon^{1/2})\text{-model stationary} \right\} \quad \forall j = 0, \dots, J.$$

For every $j = 0, \dots, J$, we have $E_j \in \mathcal{F}_{k+j}$ and $I_{k+j} \in \mathcal{F}_{k+j}$ (where I_j is the event introduced in [Definition 3.2](#)). Moreover, the events E_j and I_{k+j} are conditionally independent:

$$\forall j = 0, \dots, J, \quad \mathbb{P}_k(E_j \cap I_{k+j} \mid \mathcal{F}_{k+j-1}) = \mathbb{P}_k(E_j \mid \mathcal{F}_{k+j-1}) \mathbb{P}_k(I_{k+j} \mid \mathcal{F}_{k+j-1}). \quad (46)$$

This conditional independence holds because $x_{k+j} \in \mathcal{F}_{k+j-1}$, and the model \hat{f}_{k+J} is constructed independently of x_{k+j} by assumption. Using these events, we can reformulate the statement of the theorem as

$$\mathbb{P}_k(E \mid E_0, \dots, E_J) \geq 1 - (1 - p)^{J+1}.$$

Now, by [Lemma 3.1](#),

$$\mathbb{P}_k(E \mid E_0, \dots, E_J) \geq \mathbb{P}_k\left(\bigcup_{0 \leq j \leq J} I_{k+j} \mid E_0, \dots, E_J\right) = 1 - \mathbb{P}_k\left(\bigcap_{0 \leq j \leq J} \bar{I}_{k+j} \mid E_0, \dots, E_J\right).$$

Thus, to obtain the desired result, it suffices to prove that

$$\mathbb{P}_k\left(\bigcap_{0 \leq j \leq J} \bar{I}_{k+j} \mid E_0, \dots, E_J\right) \leq (1 - p)^{J+1}. \quad (47)$$

We now make use of the probabilistically accuracy property. For every $j = 0, \dots, J$, we have

$$\mathbb{P}_k(I_{k+j}|A) \geq p, \quad (48)$$

for any set of events A belonging to the σ -algebra \mathcal{F}_{k+j-1} [21, Chapter 5]. In particular, for any $j \geq 1$, $\mathbb{P}_k(I_{k+j}|I_k, \dots, I_{k+j-1}, E_0, \dots, E_j) \geq p$. Returning to our target probability, we have:

$$\begin{aligned} \mathbb{P}_k \left(\bigcap_{0 \leq j \leq J} \bar{I}_{k+j} \middle| E_0, \dots, E_J \right) &= \frac{\mathbb{P}_k \left(\left\{ \bigcap_{0 \leq j \leq J} \bar{I}_{k+j} \right\} \cap E_J \middle| E_0, \dots, E_{J-1} \right)}{\mathbb{P}_k(E_J|E_0, \dots, E_{J-1})} \\ &= \frac{\mathbb{P}_k(\bar{I}_J \cap E_J | E_0, \dots, E_{J-1}, I_k, \dots, I_{k+J-1}) \mathbb{P}_k(\bigcap_{0 \leq j \leq J-1} \bar{I}_{k+j} | E_0, \dots, E_{J-1})}{\mathbb{P}_k(E_J|E_0, \dots, E_{J-1})} \\ &= \frac{\mathbb{P}_k(\bar{I}_J | E_0, \dots, E_{J-1}, I_k, \dots, I_{k+J-1}) \mathbb{P}_k(\bigcap_{0 \leq j \leq J-1} \bar{I}_{k+j} | E_0, \dots, E_{J-1}) \mathbb{P}_k(E_J | E_0, \dots, E_{J-1}, I_k, \dots, I_{k+J-1})}{\mathbb{P}_k(E_J|E_0, \dots, E_{J-1})} \\ &\leq \mathbb{P}_k(\bar{I}_J | E_0, \dots, E_{J-1}, I_k, \dots, I_{k+J-1}) \mathbb{P}_k(\bigcap_{0 \leq j \leq J-1} \bar{I}_{k+j} | E_0, \dots, E_{J-1}), \end{aligned}$$

where the last equality comes from (46), and the final inequality uses the fact that the events E_0, \dots, E_{J-1} and I_k, \dots, I_{k+J-1} are pairwise independent, thus

$$\mathbb{P}_k(E_J|E_0, \dots, E_{J-1}, I_k, \dots, I_{k+J-1}) = \mathbb{P}_k(E_J|E_0, \dots, E_{J-1}).$$

Using (48), we then have that

$$\mathbb{P}_k(\bar{I}_J | E_0, \dots, E_{J-1}, I_k, \dots, I_{k+J-1}) = 1 - \mathbb{P}_k(I_J | E_0, \dots, E_{J-1}, I_k, \dots, I_{k+J-1}) \leq 1 - p.$$

Thus,

$$\mathbb{P}_k \left(\bigcap_{0 \leq j \leq J} \bar{I}_{k+j} \middle| E_0, \dots, E_J \right) \leq (1-p) \mathbb{P}_k \left(\bigcap_{0 \leq j \leq J-1} \bar{I}_{k+j} \middle| E_0, \dots, E_{J-1} \right). \quad (49)$$

By a recursive argument on the right-hand side of (49), we thus arrive at (47), which yields the desired conclusion.

A.5 Proof of Proposition 4.2

As in Theorem 4.3, $T_{\epsilon, J}^m$ clearly is a stopping time. Moreover, if $\pi_k = 1$ for all k , then $T_{\epsilon, J}^m = T_\epsilon$ for every J , where T_ϵ is the stopping time defined in Theorem 4.3, and therefore the result holds. In what follows, we thus focus on the remaining case.

Consider an iterate k such that x_k is $(\hat{\epsilon}, \hat{\epsilon}^{1/2})$ -function stationary and the model \hat{f}_k is accurate. From the definition of $\hat{\epsilon}$, such an iterate is also $((1 - \kappa_g)\epsilon, (1 - \kappa_H)\epsilon^{1/2})$ -function stationary and the model \hat{f}_k is accurate. Then, by a reasoning similar to that of the proof of Lemma 3.1, we can show that x_k is $(\epsilon, \epsilon^{1/2})$ -model stationary. As a result, if $T_{\epsilon, J}^m > k$, one of the models $\hat{f}_k, \hat{f}_{k+1}, \dots, \hat{f}_{k+J}$ must be inaccurate, which happens with probability $1 - p^{J+1}$.

Let $T_{\epsilon, J}$ be the first iteration index for which the iterate is a $(\hat{\epsilon}, \hat{\epsilon}^{1/2})$ function stationary point and satisfies (33), i. e.

$$\min\{\|g_k\|, \|g_k^+\|\} < \epsilon \quad \text{and} \quad \lambda_k > -\epsilon^{1/2}, \quad \forall k \in \{T_{\epsilon, J}^m, T_{\epsilon, J}^m + 1, \dots, T_{\epsilon, J}^m + J\}.$$

Clearly $T_{\epsilon, J}^m \leq T_{\epsilon, J}$ (for all realizations of these two stopping times), and it thus suffices to bound $T_{\epsilon, J}$ in expectation. By applying Theorem 4.3 (with ϵ in the theorem's statement replaced by

$\hat{\epsilon}$), one can see that there must exist an infinite number of $(\hat{\epsilon}, \hat{\epsilon}^{1/2})$ -function stationary points in expectation. More precisely, letting $\{T_{\hat{\epsilon}}^{(i)}\}_{i=1, \dots}$ be the corresponding stopping times indicating the iteration indexes of these points and using Theorem 4.3, we have

$$\begin{aligned} \mathbb{E} [T_{\hat{\epsilon}}^{(1)}] &= \mathbb{E} [T_{\hat{\epsilon}}] \leq \frac{(f(x_0) - f_{\text{low}})}{p\hat{c}} \hat{\epsilon}^{-3/2} + 1, \\ \forall i \geq 1, \quad \mathbb{E} [T_{\hat{\epsilon}}^{(i+1)} - T_{\hat{\epsilon}}^{(i)}] &\leq \frac{(f(x_0) - f_{\text{low}})}{p\hat{c}} \hat{\epsilon}^{-3/2} + 1. \end{aligned}$$

Consider now the subsequence $\{T_{\hat{\epsilon}}^{(i_\ell)}\}_{\ell=1, \dots}$ such that all stopping times are at least J iterations from each other, i.e., for every $\ell \geq 1$, we have $T_{\hat{\epsilon}}^{(i_{\ell+1})} - T_{\hat{\epsilon}}^{(i_\ell)} \geq J$. For such a sequence, we get

$$\begin{aligned} \forall \ell \geq 1, \quad \mathbb{E} [T_{\hat{\epsilon}}^{(i_{\ell+1})} - T_{\hat{\epsilon}}^{(i_\ell)}] &\leq \frac{(f(x_0) - f_{\text{low}})}{p\hat{c}} \hat{\epsilon}^{-3/2} + J + 1 \triangleq K(\epsilon, J) \\ \mathbb{E} [T_{\hat{\epsilon}}^{(i_1)}] &= \mathbb{E} [T_{\hat{\epsilon}}] \leq \frac{(f(x_0) - f_{\text{low}})}{p\hat{c}} \hat{\epsilon}^{-3/2} + 1 \leq K(\epsilon, J). \end{aligned}$$

For every $\ell \geq 1$, we define the event

$$B_\ell = \bigcap_{j=0}^J I_{T_{\hat{\epsilon}}^{(i_\ell)} + j} = \bigcap_{j=0}^J \left\{ m_{T_{\hat{\epsilon}}^{(i_\ell)} + j} \text{ is accurate} \right\}.$$

By Assumption 4.1, the samples are generated independently of the current iterate, and for every k , $\mathbb{P}(I_k | \mathcal{F}_{k-1}) = p$. By the same recursive reasoning as in the proof of Proposition 4.1, we have that $\mathbb{P} \left(B_\ell | \mathcal{F}_{T_{\hat{\epsilon}}^{(i_\ell)} - 1} \right) = p^{J+1}$. Moreover, by definition of the sequence $\{T_{\hat{\epsilon}}^{(i_\ell)}\}$, two stopping times in that sequence correspond to two iteration indexes distant of at least $J+1$. Therefore, they also correspond to two separate sequences of $(J+1)$ models that are generated in an independent fashion. We can thus consider $\{B_\ell\}$ to be an independent sequence of Bernoulli trials. Therefore, the variable G representing the number of runs of B_ℓ until success follows a geometric distribution with an expectation less than $\frac{1}{p^{J+1}} = p^{-(J+1)} < \infty$. On the other hand, $T_{\epsilon, J}$ is less than the first element of $\{T_{\hat{\epsilon}}^{(i_\ell)}\}$ for which B_ℓ happens, and thus $T_{\epsilon, J} \leq T_{\hat{\epsilon}}^{(i_G)}$. To conclude the proof, we define

$$S_G = T_{\hat{\epsilon}}^{(i_G)}, \quad X_1 = T_{\hat{\epsilon}}^{(i_1)} = T_{\hat{\epsilon}}^1, \quad X_\ell = T_{\hat{\epsilon}}^{(i_\ell)} - T_{\hat{\epsilon}}^{(i_{\ell-1})} \quad \forall \ell \geq 2.$$

From the proof of Wald's equation [21, Theorem 4.1.5] (more precisely, from the third equation appearing in that proof), one has

$$\mathbb{E} [S_G] = \sum_{\ell=1}^{\infty} \mathbb{E} [X_\ell] \mathbb{P}(G \geq \ell).$$

Since $\mathbb{E} [X_\ell] \leq K(\epsilon, J)$, one arrives at

$$\mathbb{E} [T_{\epsilon, J}^m] \leq \mathbb{E} [T_{\epsilon, J}] \leq \mathbb{E} [T_{\hat{\epsilon}}^{(i_G)}] \leq K(\epsilon, J) \sum_{\ell=1}^{\infty} \mathbb{P}(G \geq \ell) = K(\epsilon, J) \mathbb{E} [G],$$

which is the desired result.

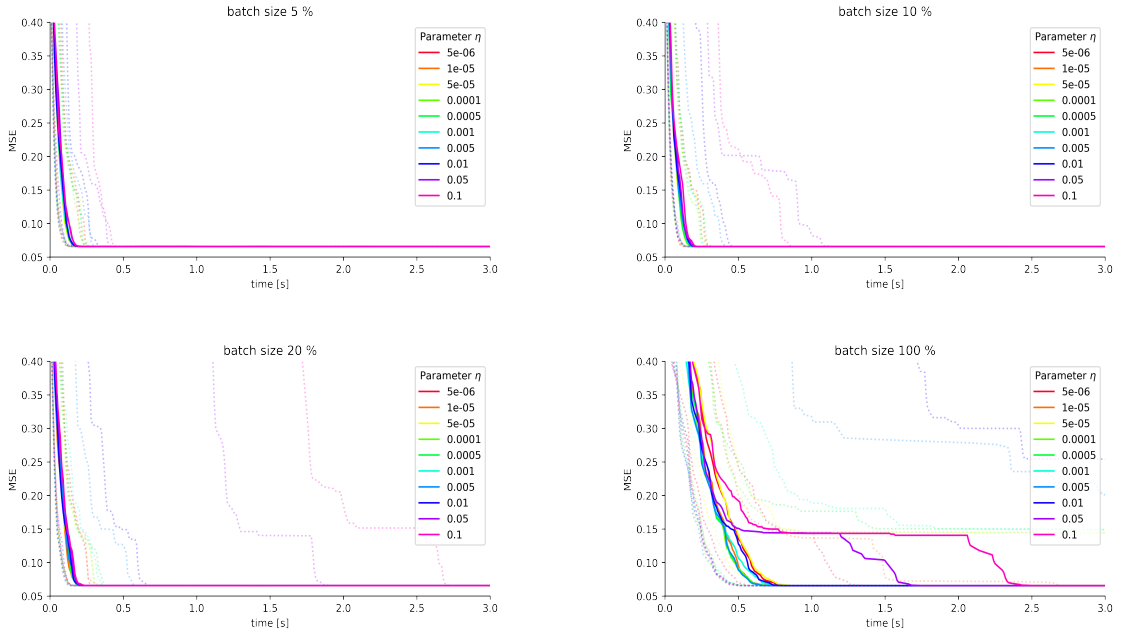


Figure 8: The sensitivity of the performance of the ALAS algorithm on the IJCNN1 task as depending on the choice of η .

B More details on numerical results

B.1 ALAS algorithm as implemented

Our implementation of the ALAS algorithm is described in Algorithm 2. The main differences between Algorithm 2 and Algorithm 1 are described in the main paper.

B.2 Distribution of Steps

IJCNN Dataset We have included most of the visual information for the runs on the IJCNN in the main part of the paper. One additional consideration to verify the stability of the algorithm is to perform a sensitivity analysis of the hyperparameters of ALAS. There are two hyperparameters in the ALAS algorithm, η and ϵ . In deterministic contexts, η is typically kept small to allow for fairly liberal step acceptance. We studied the impact of varying this hyperparameter on the performance of ALAS, reporting our results in Figure 8. We confirm that indeed for reasonably small values the precise value has limited impact on the convergence. This is by contrast with SGD wherein the learning rate has a very significant impact on the performance and typically has to be tuned for each problem. The sensitivity of the Algorithm with respect to ϵ is shown in Figure 9. It can be seen that here, as well, the Algorithm is not particularly sensitive. Although the Regularized Newton step, which depends on ϵ explicitly, is chosen the most, it appears that it is modified in an appropriate space so as to mitigate any degradation of performance.

Algorithm 2: ALAS, as implemented.

Initialization: Choose $x_0 \in \mathbb{R}^n$, $\theta \in (0, 1)$, $\eta > 0$, $\epsilon > 0$.

for $k = 0, 1, \dots$ **do**

1. Draw a random sample set $\mathcal{S}_k \subset \{1, \dots, N\}$, and compute the associated quantities $g_k := g(x_k; \mathcal{S}_k)$, $H_k := H(x_k; \mathcal{S}_k)$. Form the model:

$$\hat{f}_k(x_k + s) := \hat{f}(x_k + s; \mathcal{S}_k). \quad (50)$$

2. Compute $R_k = \frac{g_k^\top H_k g_k}{\|g_k\|^2}$.

3. If $R_k < -\|g_k\|^{1/2}$ then set $d_k = \frac{R_k}{\|g_k\|} g_k$ and go to the Line-search step.

4. Else if $R_k < \|g_k\|^{1/2}$ and $\|g_k\| \geq \epsilon$ then set $d_k = -\frac{g_k}{\|g_k\|^{1/2}}$ and go to the Line-search step.

5. Compute λ_k as the minimum eigenvalue of the Hessian estimate H_k .
If $\lambda_k \geq -\epsilon^{1/2}$ and $\|g_k\| = 0$ set $\alpha_k = 0$, $d_k = 0$ and go to Step 10.

6. If $\lambda_k < -\|g_k\|^{1/2}$, Compute a negative eigenvector v_k such that

$$H_k v_k = \lambda_k v_k, \quad \|v_k\| = -\lambda_k, \quad v_k^\top g_k \leq 0, \quad (51)$$

set $d_k = v_k$ and go to the line-search step.

7. If $\lambda_k > \|g_k\|^{1/2}$, compute a Newton direction d_k solution of

$$H_k d_k = -g_k, \quad (52)$$

go to the line-search step.

8. If d_k has not yet been chosen, compute it as a regularized Newton direction, solution of

$$\left(H_k + (\|g_k\|^{1/2} + \epsilon^{1/2}) \mathbb{I}_n \right) d_k = -g_k, \quad (53)$$

and go to the line-search step.

9. **Line-search step** Compute the minimum index j_k such that the step length $\alpha_k := \theta^{j_k}$ satisfies the decrease condition:

$$\hat{f}_k(x_k + \alpha_k d_k) - \hat{f}_k(x_k) \leq -\frac{\eta}{2} \alpha_k^2 \|d_k\|^2. \quad (54)$$

10. Set $x_{k+1} = x_k + \alpha_k d_k$.

11. Set $k = k + 1$.

end

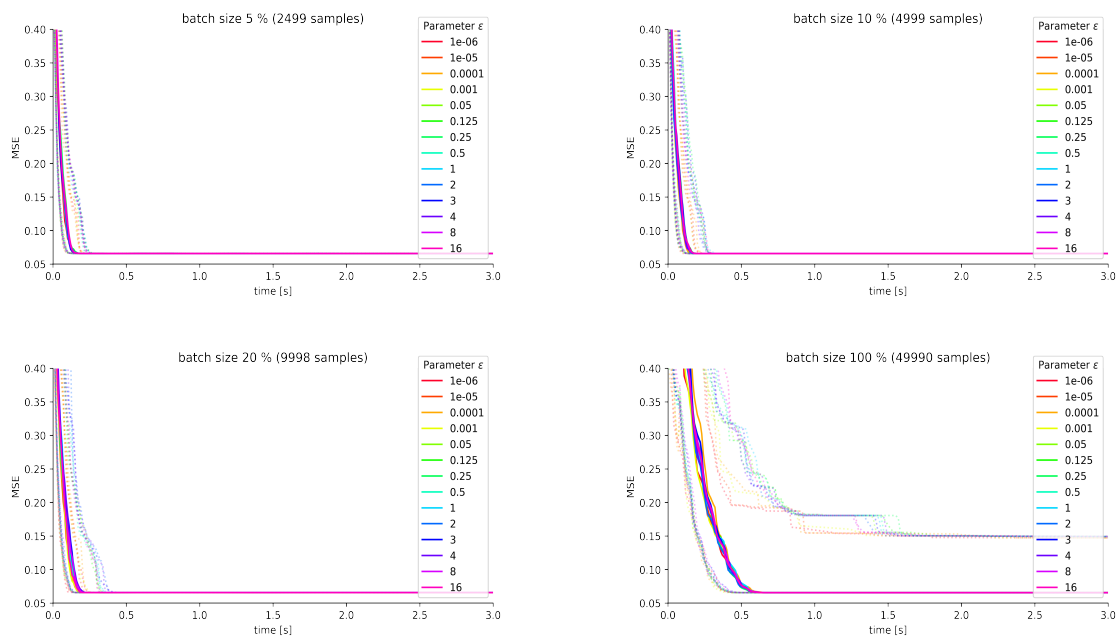


Figure 9: The sensitivity of the performance of the ALAS algorithm on the IJCNN1 task as depending on the choice of ϵ .

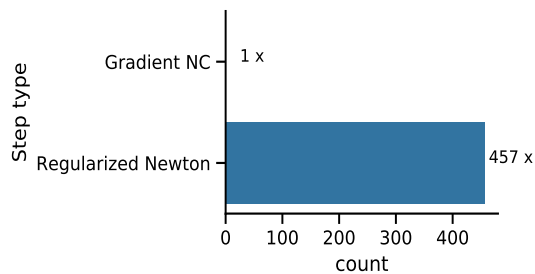
A9A Dataset The distribution of the individual type of steps as described in Algorithm 2 for selected runs for the A9A task is shown in Figure 10. As in the case of IJCNN1 task, the most frequently used step type is the *Regularized Newton*. We note that when a full sample is used, *Negative curvature* steps are more common, suggesting that the problem is quite nonconvex. Note that in all of our runs (including those not reported here), other step choices were used less than 10 times. The distributions of number of line-search iterations for selected runs of the ALAS algorithm are shown in Figure 11.

MNIST Transfer Learning The distribution of the individual type of steps as described in Algorithm 2 for selected runs for the transfer learning task is shown in Figure 12. Again, the most frequently used step type was the *Regularized Newton* and the others occurred very rarely. The distribution of the number of line-search iterations for selected runs of the ALAS algorithm are shown in Figure 13; the line search was usually rather short (0 iterations of were dominating for most runs) but it was still used quite often.

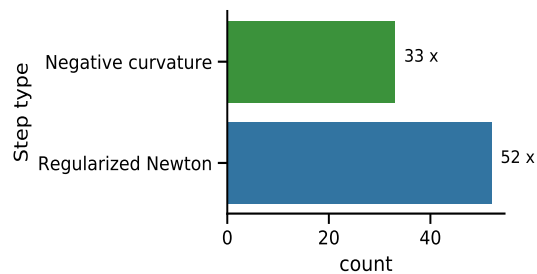
Artificial NN The step type distribution for different runs is shown in Figure 14 — the most frequent steps in general for this task were the *Regularized Newton* (strongly dominating) and the *Negative curvature* step.

B.3 Additional plots for IJCNN1

We tested SGD with several possible values for the learning rate, namely 1, 0.6, 0.3, 0.1, 0.01, 0.001. Figure 15 shows the performance of a subset of those values: as one may expect, SGD is

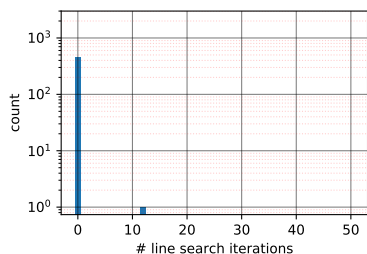


(a) 123-1 5%

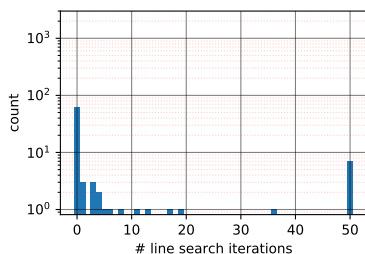


(b) 123-1 100%

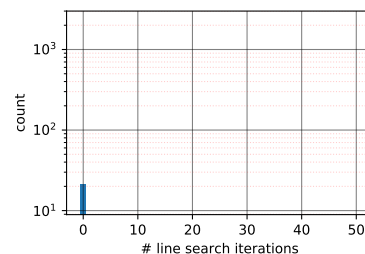
Figure 10: The step type distribution of a single run of ALAS algorithm on the A9A task for the 123-1 architecture and two sampling sizes.



(a) 123-1 5%

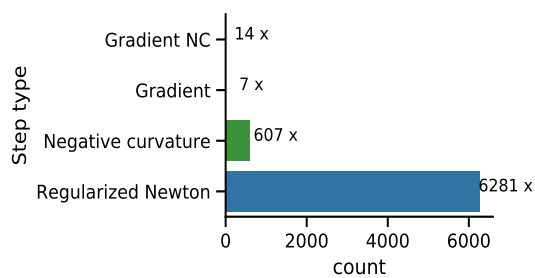


(b) 123-1 100%

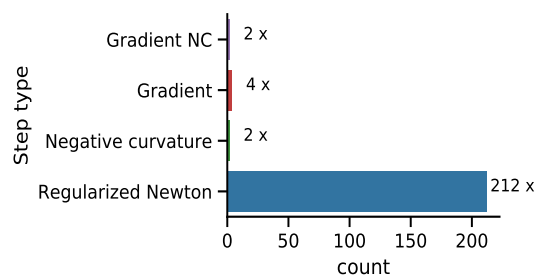


(c) 123-2-1 100%

Figure 11: Plots of the number of line-search iterations during each update for the A9A task for selected runs of the ALAS algorithm with different architectures and sampling sizes. The maximum number of line-search iterations was set to 50.



(a) 8-2-1 5%



(b) 8-4-1 100%

Figure 12: The step type distribution of a single run of ALAS algorithm on the transfer learning task.

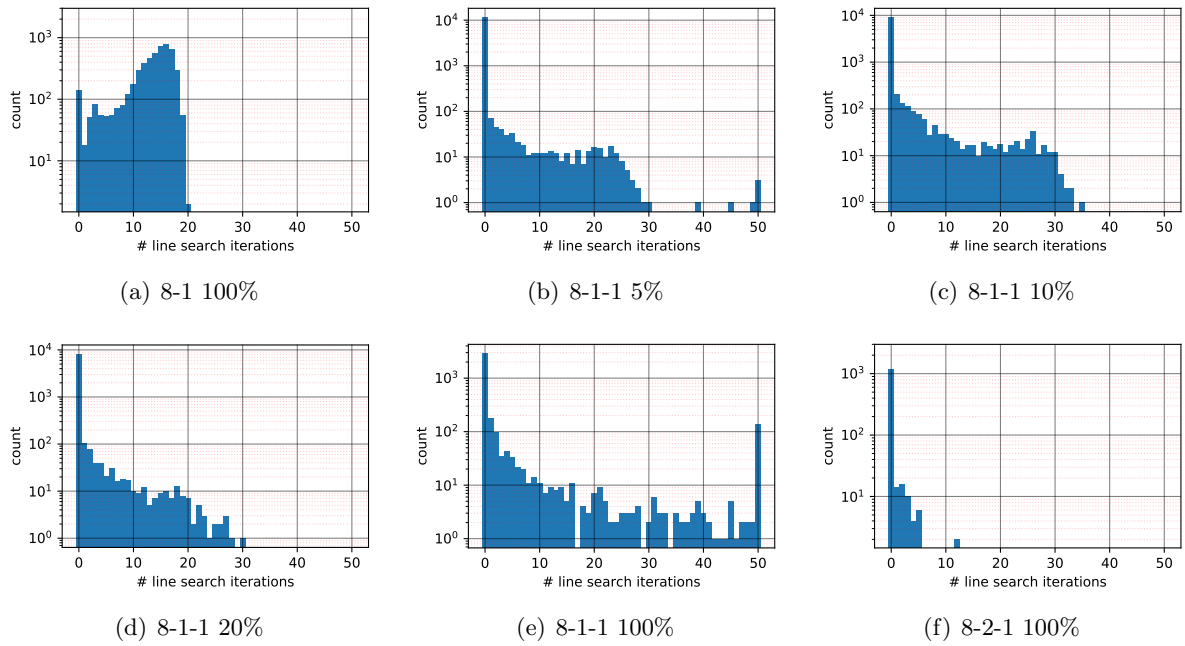


Figure 13: Plots of the number of line-search iterations during each update for the transfer learning task for selected runs of the ALAS algorithm with different architectures and sampling sizes. The maximum number of line-search iterations was set to 50.

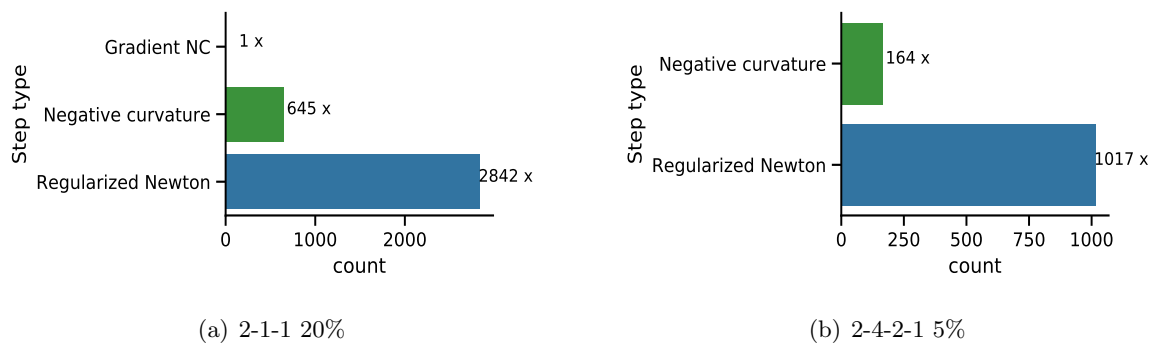


Figure 14: The step type distribution of a single run of ALAS algorithm on the NN1 task.

quite sensitive to the choice of the step size.

C Additional numerical experiments

C.1 Experiment using the A9A dataset

The second set of experiments was run on the A9A training dataset, also part of the LIBSVM library [17]: for this classification dataset, we have $N = 32,561$ samples, each of them possessing $n = 123$ features. For this task, we trained two neural networks without hidden layers and with one hidden layer having a single neuron; the optimized function was the MSE as in the first experiment. Our batch sizes consisted of 100%, 20%, 10% and 5% of the dataset size, and the mean-squared error loss was used. We tested four variants of SGD corresponding to the values 1, 0.6, 0.3, 0.1 for the learning rate, and selected the best variant for comparison with ALAS. The results are shown in Figures 16 and 17, as well as Table 4. Our method, ALAS, was significantly better for all sampling sizes on training the first network. However, for the second network with more optimization variables (learning parameters), ALAS appears to slow down relative to SGD. This appears due to our use of exact linear algebra techniques: as explained in the introduction of this section, the results could be better for an inexact variant of ALAS.

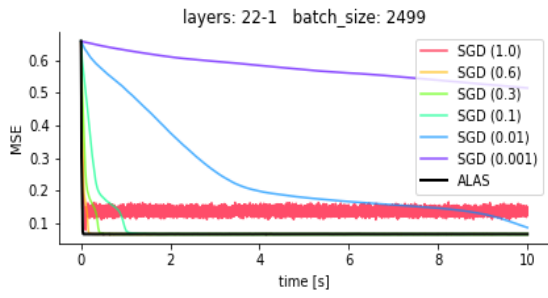
Layers: 123-1					Layers: 123-2-1				
alg.	π_k	min loss	loss [8-10]s	iter.	alg.	π_k	min loss	loss [8-10]s	iter.
ALAS	5%	0.1176	0.1182	458	ALAS	5 %	0.1428	0.1437	20
SGD (0.1)	5%	0.1224	0.1231	8260	SGD (0.6)	5 %	0.1066	0.1085	5992
ALAS	10 %	0.1168	0.1176	360	ALAS	10 %	0.1464	0.1482	13
SGD (0.1)	10 %	0.1245	0.1255	6168	SGD (0.6)	10 %	0.1094	0.1129	3948
ALAS	20 %	0.1163	0.1171	255	ALAS	20 %	0.1436	0.1452	14
SGD (0.1)	20 %	0.1396	0.1482	4152	SGD (0.6)	20%	0.1163	0.1213	2449
ALAS	100 %	0.1151	0.1151	85	ALAS	100 %	0.1550	0.1579	6
SGD (0.3)	100 %	0.2157	0.2786	645	SGD (0.6)	100 %	0.1353	0.1365	819

Table 4: Results reached over the given time period $t = 10$ s on the A9A task.

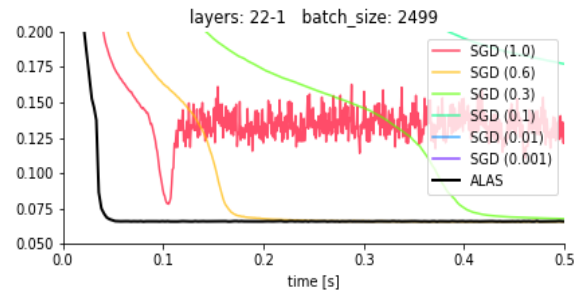
C.2 An artificial dataset

To illustrate the performance of ALAS on highly non-linear problems, we have created two artificial datasets, the first of which (thereafter called NN1) was generated using a neural network with random weights sampled from a normal distribution ($w_i \in \mathcal{N}(0, 3)$) and two input neurons, two hidden layers with four and two neurons, respectively. We use hyperbolic tangent activation functions in all layers. To produce the actual training data, 50,000 points were sampled from a uniform distribution ($\vec{x}_i \in \mathcal{R}^2, x_{ij} \in \mathcal{U}(0, 1)$) and passed through the generated network to produce target values $\{y_i\}_i$.

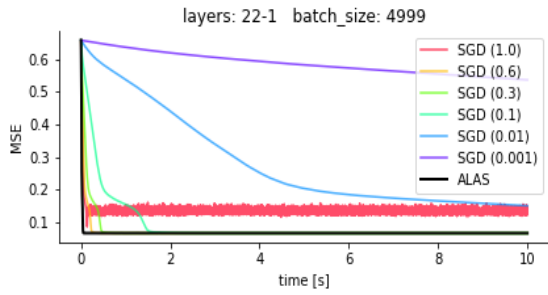
The optimization task was then to reconstruct the target values $\{y_i\}_i$ from the generated points $\{\vec{x}_i\}_i$ using different neural networks using the MSE as the loss function. We tried the values 1, 0.6, 0.3, 0.1 for the learning rate of SGD, and we compared these variants with ALAS, using 100%, 20 %, 10 %, and 5% of the sample sizes. The results are shown in Table 5: the algorithm ALAS performed best with a single exception when it got stuck in a worse local optimum than the SGD variant.



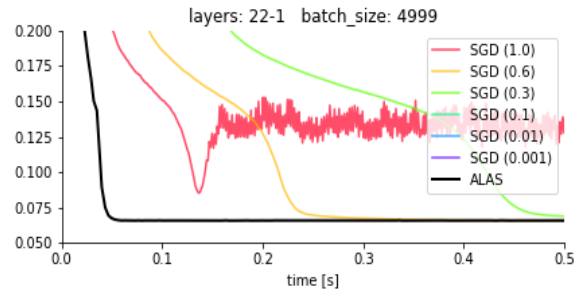
(a) 22-1 5%



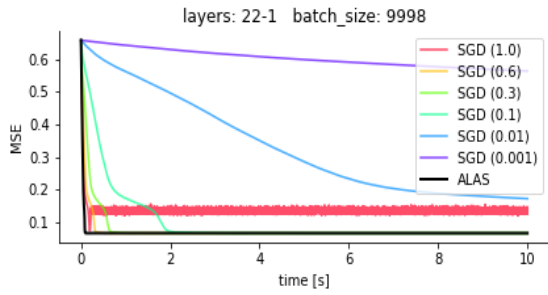
(b) 22-1 5% (zoom)



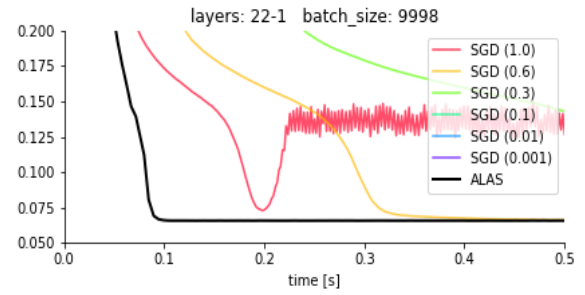
(c) 22-1 10%



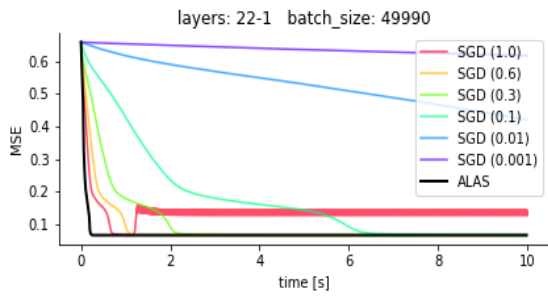
(d) 22-1 10% (zoom)



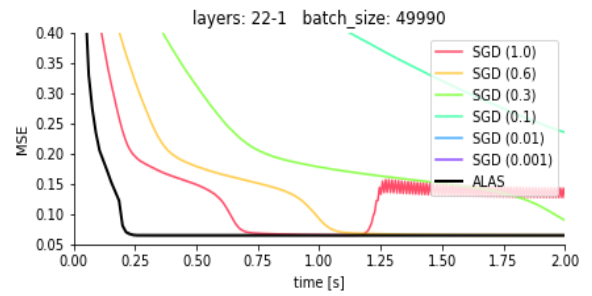
(e) 22-1 20%



(f) 22-1 20% (zoom)



(g) 22-1 100%



(h) 22-1 100% (zoom)

Figure 15: Comparison of ALAS and SGD (with various learning rates) on the IJCNN1 dataset.

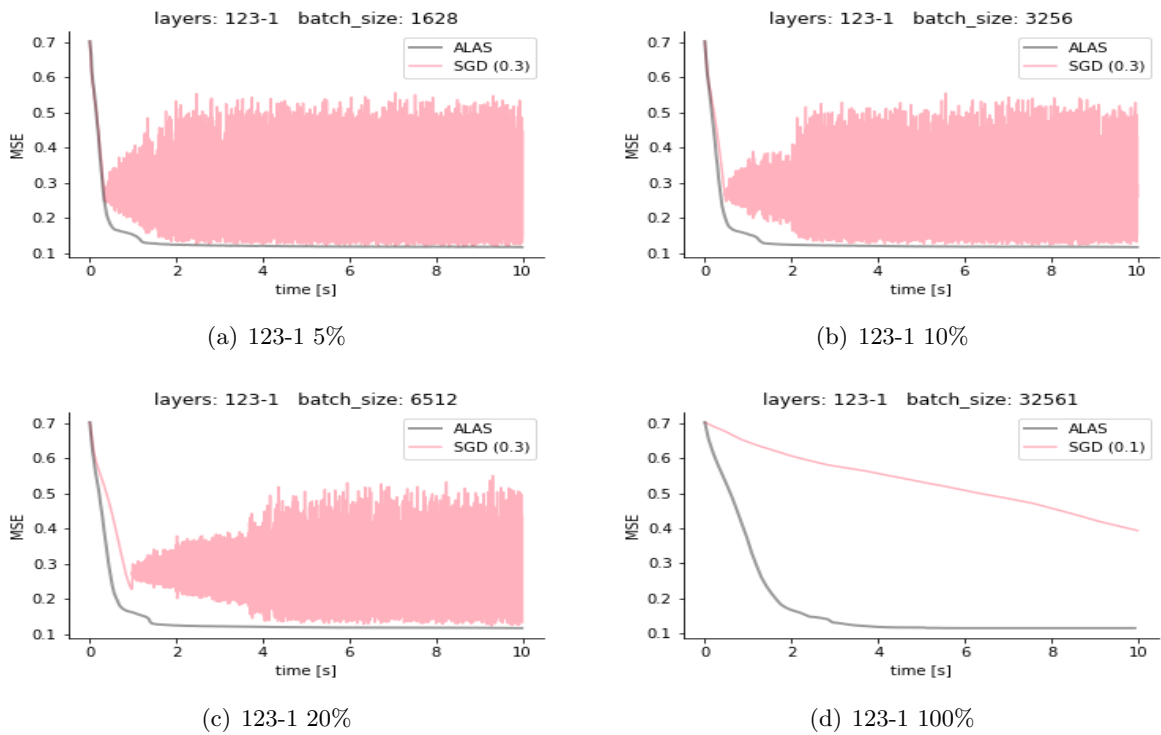


Figure 16: Comparison of ALAS and SGD (with best performing learning rate) on the A9A dataset with a simple neural network with 123 input neurons, no hidden layer and an output neuron.

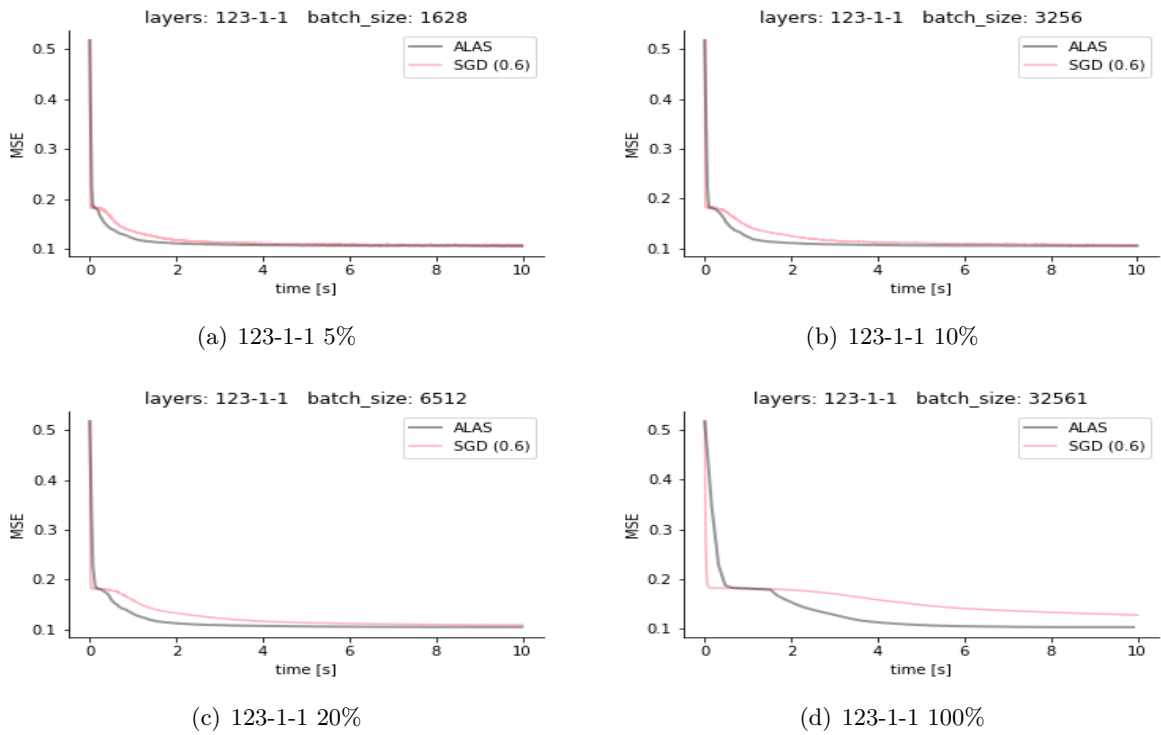


Figure 17: Comparison of ALAS and SGD (with best performing learning rate) on the A9A dataset with a simple neural network with 123 input neurons, hidden layer with a single neuron and an output neuron.

Layers: 2-1-1					Layers: 2-2-1				
alg.	π_k	min loss	loss [8-10]s	iter.	alg.	π_k	min loss	loss [8-10]s	iter.
ALAS	5%	9.08e-10	1.12e-9	7471	ALAS	5%	6.59e-10	4.000	5736
SGD (1.0)	5%	2.49e-6	2.76e-6	15432	SGD (1.0)	5%	1.60e-6	1.78e-6	14105
ALAS	10%	8.94e-10	1.01e-9	5595	ALAS	10%	1.59e-10	2.18e-10	2352
SGD (1.0)	10%	2.77e-6	3.09e-6	14015	SGD (1.0)	10%	1.86e-6	2.07e-6	12134
ALAS	20%	8.91e-10	9.39e-10	3353	ALAS	20%	1.96e-10	2.23e-10	1267
SGD (1.0)	20%	3.41e-6	3.80e-6	11533	SGD (1.0)	20%	2.20e-6	2.44e-6	10283
ALAS	100%	1.15e-9	1.211e-9	538	ALAS	100%	9.62e-10	9.99e-10	304
SGD (1.0)	100%	7.51e-6	8.42e-6	5503	SGD (1.0)	100%	5.99e-6	6.68e-6	3833
Layers: 2-4-1-1					Layers: 2-4-2-1				
ALAS	5%	9.21e-10	9.23e-10	1529	ALAS	5%	9.27e-10	9.34e-10	922
SGD (1.0)	5%	5.47e-7	5.60e-7	13224	SGD (1.0)	5%	1.68e-6	1.86e-6	11909
ALAS	10%	9.94e-10	1.03e-9	818	ALAS	10%	1.03e-9	1.05e-9	493
SGD (1.0)	10%	5.75e-7	5.88e-7	10873	SGD (1.0)	10%	2.17e-6	2.39e-6	9192
ALAS	20%	1.26e-9	1.34e-9	485	ALAS	20%	1.25e-9	1.30e-9	262
SGD (1.0)	20%	6.03e-7	6.12e-7	8223	SGD (1.0)	20%	2.91e-6	3.20e-6	6850
ALAS	100%	4.05e-9	4.43e-9	94	ALAS	100%	3.59e-9	3.96e-9	55
SGD (1.0)	100%	6.76e-7	6.80e-7	2819	SGD (1.0)	100%	9.76e-6	1.09e-5	2008

Table 5: Results reached over the given time period $t = 10$ s on the artificial dataset NN1.

C.3 A second artificial dataset

The second artificial dataset, called NN2, was created using the same process as described in the main paper for the first. For this second dataset, we used a deeper neural network in order to introduce more nonlinearities: this network consisted of four input neurons, three hidden layers with up to four neurons, and one output layer producing the targets $\{y_i\}_i$. The networks used for experiments had one or two hidden layers — first hidden layer had always four neurons and the second had one or two neurons if present. All neurons used a hyperbolic tangent as their activation function, the optimized function was the MSE. Few runs of the ALAS and the SGD algorithms are shown in Figures 18 and 19. The step type distribution for different runs is shown in Figure 20 — the *Regularized Newton* step type was the most frequent. Our implementation of ALAS performed generally better than the best SGD variant, sometimes by a significant margin.

Layers: 4-4-1					Layers: 4-4-2-1				
alg.	π_k	min loss	loss [8-10]s	iter.	alg.	π_k	min loss	loss [8-10]s	iter.
ALAS	5%	0.0153	0.0163	1654	ALAS	5%	0.0150	0.0154	1046
SGD (1.0)	5%	0.0411	0.0466	13185	SGD (1.0)	5%	0.0167	0.0222	11814
ALAS	10%	0.0145	0.0156	1218	ALAS	10%	0.0160	0.0161	650
SGD (1.0)	10%	0.0466	0.0513	10548	SGD (1.0)	10%	0.0185	0.0260	8764
ALAS	20%	0.0158	0.0168	727	ALAS	20%	0.0159	0.0160	320
SGD (1.0)	20%	0.0527	0.0562	7617	SGD (1.0)	20%	0.0242	0.0317	6123
ALAS	100%	0.0122	0.0133	126	ALAS	100%	0.0148	0.0153	69
SGD (1.0)	100%	0.0646	0.0651	3068	SGD (1.0)	100%	0.0384	0.0489	2222

Table 6: The comparison of the minimal (full) losses reached over the given time period $t = 10$ s on the artificial dataset NN2. The number in the parenthesis for SGD entries is the step size. The column $loss [8-10]s$ shows the median loss over the last two seconds.

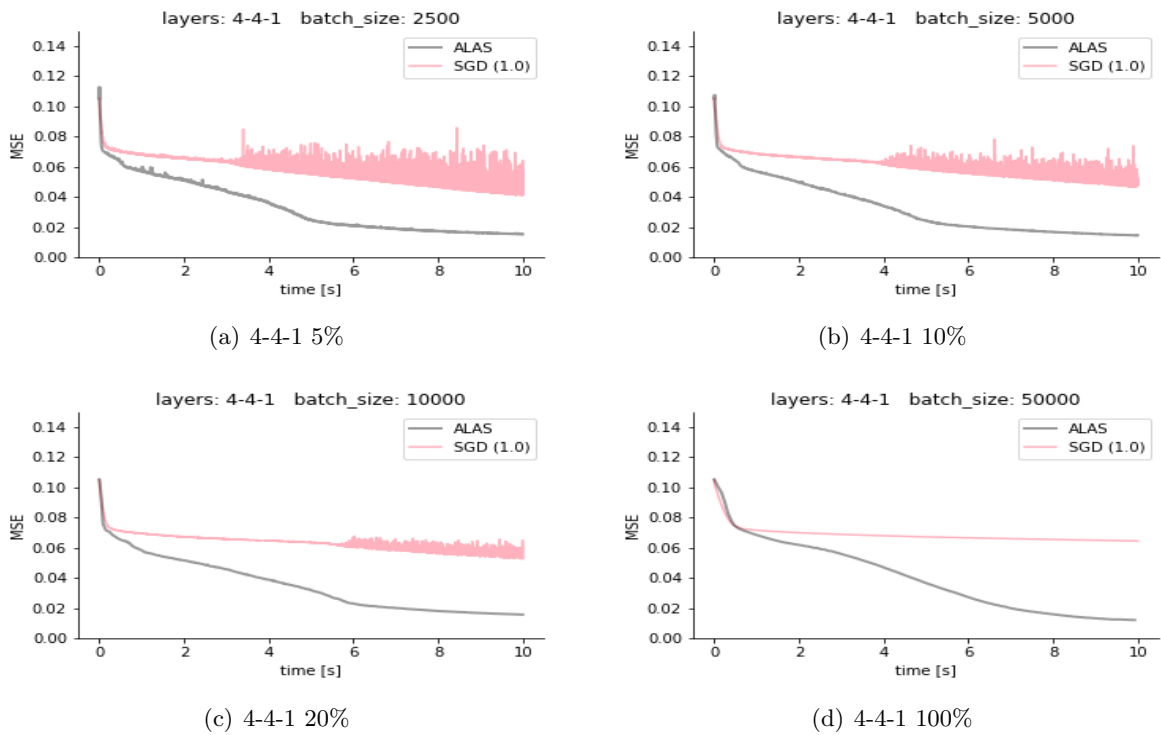


Figure 18: Evaluation of the ALAS algorithm on artificial task NN2 compared to the SGD with best performing learning rate. Full losses are depicted.

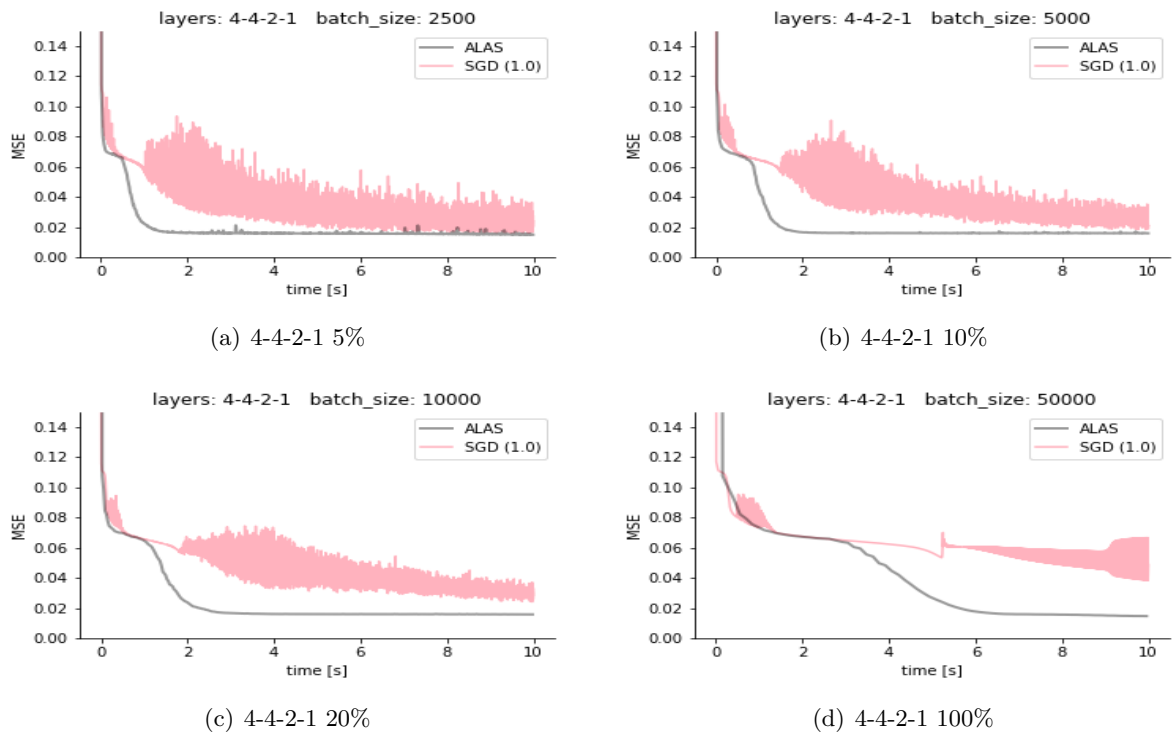


Figure 19: Evaluation of the ALAS algorithm on artificial task NN2 compared to the SGD with best performing learning rate. Full losses are depicted.

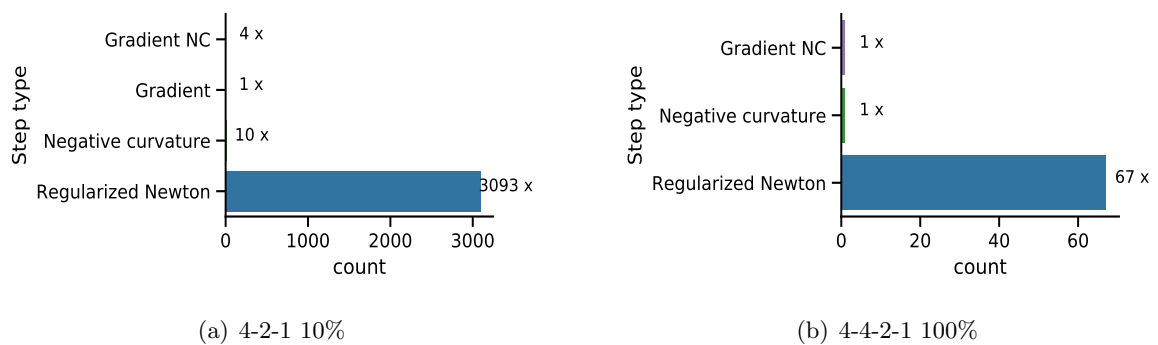


Figure 20: The step type distribution of a single run of ALAS algorithm on the NN2 task.